25. Chen J J, Sun Y, Nabel G J. Regulation of the proinflammatory effects of Fas ligand (CD95L). Science 1998; 282: 1714–7.
26. Bellgrau D, Gold D, Selawry H, et al. A role for CD95 ligand in preventing graft rejection. Nature 1995; 377: 630–2.
27. Schmidt C, Bladt F, Goedecke S, et al. Scatter factor/hepatocyte growth factor is essential for liver development. Nature 1995; 373: 699–702.
28. Ueki T, Kaneda Y, Tsutsumi H, et al. Hepatocyte growth factor gene therapy of liver cirrhosis in rats. Nat Med 1999; 5: 226–30.
29. Ajioka I, Akaike T, Watanabe Y. Expression of vascular endothelial growth factor promotes colonization, vascularization, and growth of transplanted hepatic tissues in the mouse. Hepatology 1999; 29: 396–402.
30. Peters M, Blinn G, Jostock T, et al. Combined interleukin 6 and soluble interleukin 6 receptor accelerates murine liver regeneration. Gastroenterology 2000; 119: 1663–71.
31. Friedman S L. Closing in on the signals of hepatic fibrosis. Gastroenterology 1997; 112: 1406–9.
32. Ohashi K, Marion P L, Nakai H, et al. Sustained survival of human hepatocytes in mice: a model for *in vivo* infection with human hepatitis B and hepatitis delta viruses. Nat Med 2000; 6: 327–31.
33. Dandri M, Burda M R, Torok E, et al. Repopulation of mouse liver with human hepatocytes and *in vivo* infection with hepatitis B virus. Hepatology 2001; 33: 981–8.
34. Shimizu Y K, Weiner A J, Rosenblatt J, et al. Early events in hepatitis C virus infection of chimpanzees. Proc Natl Acad Sci USA 1990; 87: 6441–4.
35. Farci P, Purcell R H. Clinical significance of hepatitis C virus genotypes and quasispecies. Semin Liver Dis 2000; 20: 103–26.
36. Farci P, Alter H J, Wong D C, et al. Prevention of hepatitis C virus infection in chimpanzees after antibody-mediated *in vitro* neutralization. Proc Natl Acad Sci USA 1994; 91: 7792–6.
37. Zhao X, Tang Z Y, Klumpp B, et al. Primary hepatocytes of Tupaia belangeri as a potential model for hepatitis C virus infection. J Clin Invest 2002; 109: 221–32.
38. Kolykhalov A A, Mihalik K, Feinstone S M, et al. Hepatitis C virus-encoded enzymatic activities and conserved RNA elements in the 3' nontranslated region are essential for virus replication *in vivo*. J Virol 2000; 74: 2046–51.
39. Neumann A U, Lam N P, Dahari H, et al. Hepatitis C viral dynamics *in vivo* and the antiviral efficacy of interferon-alpha therapy. Science 1998; 282: 103–7.
40. Lerat H, Berby F, Trabaud M A, et al. Specific detection of hepatitis C virus minus strand RNA in hematopoietic cells. J Clin Invest 1996; 97: 845–51.
41. Agnello V, Abel G, Knight G B, et al. Detection of widespread hepatocyte infection in chronic hepatitis C. Hepatology 1998; 28: 573–84.
42. Rubbia-Brandt L, Quadri R, Abid K, et al. Hepatocyte steatosis is a cytopathic effect of hepatitis C virus genotype 3. J Hepatol 2000; 33: 106–15.

Pathology International 2004; **54**: 285–294

Original Article

Tumor angiogenesis in the bone marrow of multiple myeloma patients and its alteration by thalidomide treatment

Wenlin Du,[1] Yutaka Hattori,[2] Akinori Hashiguchi,[1] Kensuke Kondoh,[1] Nobumichi Hozumi,[3] Yasuo Ikeda,[2] Michiie Sakamoto,[1] Jun-ichi Hata[4] and Taketo Yamada[1]

Departments of [1]Pathology and [2]Hematology, Keio University School of Medicine, [4]National Center for Child Health and Development, Tokyo and [3]Institute for Biological Sciences, Science University of Tokyo, Chiba, Japan

Angiogenesis in solid tumors is important to tumor growth, invasion and metastasis. Recently, it has been suggested that angiogenesis plays a certain role in the development of hematopoietic malignancies, including leukemia and multiple myeloma. We evaluated tumor angiogenesis in the bone marrow (BM) of multiple myeloma (MM) patients by calculating microvessel density (MVD) in needle-biopsy specimens obtained from 51 cases of untreated MM or monoclonal gammopathy of undetermined significance (MGUS). The MVD in the BM of donors for transplantation and patients with non-hematological diseases was calculated as a control. There was an obvious increase in MVD in the BM of MM patients, and the MVD correlated with the grade of myeloma cell invasion of the BM in the untreated MM cases. It was recently reported that thalidomide might be effective for the treatment of MM. We assessed the effect of thalidomide on angiogenesis in BM treatment of 11 patients with refractory MM. The concentration of M-protein in the serum or urine of seven of the 11 patients was reduced by at least 30% after thalidomide treatment, and MVD in the BM decreased in three of these seven cases in response to thalidomide. Increased plasma concentrations of basic fibroblast growth factor (FGF-2) and vascular endothelial growth factor (VEGF) were observed in all 11 cases before thalidomide administration and both levels were reduced after treatment with thalidomide. Augmented angiogenesis in the bone marrow of MM patients was confirmed in the present study. It seems that thalidomide is effective in the treatment of MM through the impairment of angiogenesis by decreasing FGF-2 and VEGF production. This is the first report on pathological evidence in the bone marrow of MM before and after thalidomide treatment, in Japan.

Key words: angiogenesis, CD34, fibroblast growth factor, multiple myeloma, thalidomide, vascular endothelial growth factor

Correspondence: Taketo Yamada, MD, Department of Pathology, Keio University School of Medicine, 35 Shinanomachi, Shinjuku-ku, Tokyo 160-8582, Japan. Email: taketo@sc.itc.keio.ac.jp

Received 3 July 2003. Accepted for publication 26 December 2003.

Multiple myeloma (MM) is a plasma cell neoplasm that originates in the bone marrow and involves the entire skeleton. The myeloma cells synthesize large amounts of complete and/or incomplete immunoglobulins, which may cause a hyperviscosity syndrome, amyloidosis, and renal failure. Multiple myeloma accounts for approximately 10% of all hematological malignancies. Chemotherapy with melphalan and/or dexamethasone is effective in some cases but relapses often occur, and relapsed MM might become refractory to conventional chemotherapy.[1]

Angiogenesis is indispensable to growth, invasion and metastasis by solid tumors and occurs in other diseases, including rheumatoid arthritis, psoriasis, scleroderma and diabetic retinopathy.[2–4] Angiogenesis has been postulated to be regulated by a balance between certain angiogenic and antiangiogenic factors. Angiogenic factors include soluble factors, such as vascular endothelial growth factor (VEGF), acid and basic fibroblast growth factor (aFGF and bFGF or FGF-2), angiopoietin-1, hepatocyte growth factor (HGF) and interleukin-8 (IL-8), and adhesion molecules, such as integrins.[5–8] Vascular endothelial growth factor is considered an important vasculogenic mediator of embryonic and postnatal angiogenesis that functions in the promotion of endothelial cell growth and/or inhibition of apoptosis.[9] Elevated VEGF concentrations have been reported in several types of metastatic cancers, suggesting that it plays a role in cancer progression.[10] FGF-2 has been reported to be a potent stimulator of angiogenesis *in vitro* and is found in the serum and/or urine of patients with several types of cancer, including leukemias.[11,12] Angiogenesis has recently been reported in hematological malignancies, such as leukemia and myelodysplastic syndromes.[11,13–18] Vacca *et al.* reported finding positive correlations between increased bone marrow microvessel density (MVD) and both the plasma-cell labeling index and disease activity in MM patients.[19] The increased plasma or serum concentrations of FGF-2 and VEGF has been observed not only in solid tumors, such as prostate

cancer and renal cancers, but also in hematological malignancies, such as acute lymphocytic leukemia, acute myeloleukemia, chronic myeloleukemia, and also MM.[11,13,18] Thus, it is critical to determine whether antiangiogenetic therapy will be useful for the treatment of hematological malignancies.

Thalidomide was introduced in the 1950s as a sedative, but was withdrawn from the market in the 1960s because of its teratogenicity.[20] Recently, thalidomide has been found to be effective against erythema nodosum leprosum,[21] graft-versus-host disease[22] and Crohn's disease.[23] An antiangiogenic function of thalidomide in a rabbit cornea micropocket assay was reported by D'Amato *et al.* in 1994.[24] Rajkumar *et al.* reported that tumor angiogenesis occurs in the bone marrow of MM patients and that thalidomide therapy improved the MM in some previously treated myeloma patients.[25]

We recently reported that the elevated level of plasma FGF-2 in MM patients correlated with increased disease activity.[26] Furthermore, we showed that thalidomide was effective for the treatment of refractory MM in Japan.[27] Hence, in the present study, we assessed the MVD of the bone marrow of untreated MM patients to confirm tumor angiogenesis in MM. We also investigated the effectiveness of thalidomide treatment for refractory MM patients and whether thalidomide administration altered tumor angiogenesis.

MATERIALS AND METHODS

Patients

To study angiogenesis in MM, we evaluated 51 bone marrow biopsy specimens from 51 untreated MM patients at Keio University Hospital. The clinical characteristics of the patients are shown in Table 1. The 51 patients consisted of 28 males and 23 females, and their median age was 62 years. Forty-two cases fulfilled the diagnostic criteria for MM of the South West Oncology Group (SWOG), and the other nine cases were diagnosed with a monoclonal gammopathy of undetermined significance (MGUS) based on the SWOG criteria.[28] The major subclass of immunoglobulin heavy chains was IgG (32 out of 51 cases). We used six bone marrow specimens, two from transplantation donors and four obtained at autopsy from patients with non-hematological diseases (pneumonia in two cases and cancer without bone marrow involvement in the other two cases).

To evaluate the effect of thalidomide on angiogenesis, we analyzed bone marrow biopsy specimens before and after thalidomide administration to 11 patients with refractory MM (six females and five males) who had been treated with conventional chemotherapy, such as vincristine, melpharan, prednisolone and dexamethasone (Table 2). Two patients also received peripheral blood stem cell transplantation and Interferon alpha (IFNα) before being treated with thalidomide. The disease of all 11 patients was categorized as Durie-Salmon stage 3 before treatment with thalidomide.[29]

Table 1 Clinical parameters of untreated patients

Number of patients	51
Average age (years)	62 (range, 37–88)
Male/Female	28/23
Subclass of Ig	
IgG	32
IgA	11
IgD	2
BJP	5
Nonsecretory	1
Stage (Durie-Salmon)	
1	15
2	6
3	21
MGUS	9

BJP, Bence Jones proteins; Ig, immunoglobulin; MGUS, monoclonal gammopathies of undetermined significance.

Immunohistochemistry

Sections of paraffin-embedded bone marrow specimens were stained by a standard indirect immunohistochemical technique with anti-CD34 mouse monoclonal antibody (Novocastra, Newcastle, UK) to highlight endothelial cells. The myeloma cells in the bone marrow were stained with antihuman plasma cell mouse monoclonal antibody (VS38c; DAKO, Glostrup, Denmark). The bone marrow specimens of the patients treated with thalidomide were also stained with anti-FGF-2 rabbit polyclonal antibody (Santa Cruz Biotechnology, Santa Cruz, CA, USA) and anti-FGF Receptor 1 rabbit polyclonal antibody generated by immunizing a rabbit with a synthetic oligopeptide of human FGF Receptor 1.[30]

Measurement of bone marrow microvessel density and the grading of myeloma cell invasion

All bone marrow biopsy specimens were evaluated for cellularity by light microscopy with a 10× power objective lens. Five areas with high cellularity were randomly selected and examined with an 80× power objective lens. Five fields were taken, with each field representing an area of 0.108 mm^2. Individual microvessels (stained brown by immunohistochemistry anti-CD34 antibody) were counted in each fields and their density was calculated.

The grade of myeloma cell invasion in the bone marrow was determined by both hematoxylin–eosin (HE) staining and immunohistochemistry with anti-VS38c antibody. Invasion was graded as 'mild' if myeloma cells accounted for less

Table 2 Summary of patients treated with thalidomide

Patient	Age (years)	Sex	Immunoglobulin type	Stage	Previous treatment
1	46	M	IgG kappa	3A	MP, VAD, ABMT, dexamethasone, MCNU-VMP
2	45	M	IgA kappa	3A	VAD, EDAP, PBSCT, IFNα, radiation
3	55	F	IgG kappa	3A	VAD, PBSCT, dexamethasone, IFNα
4	57	F	BJP lamda	3B	L-PAM + ADR + dexamethasone, VAD
5	58	M	IgG kappa	3A	VAD, VCAP
6	58	M	IgA lamda	3A	VAD, dexamethasone, MP, VP-16
7	70	F	IgG kappa	3A	Dexamethasone, VCAP
8	70	F	IgG kappa	3A	Dexamethasone, melphalan, VCAP
9	63	F	IgG kappa	3A	MP, VAD
10	59	M	IgA kappa	3A	VAD, dexamethasone, VCAP
11	55	F	IgA lamda	3A	Dexamethasone, VCAP, VCAD

AMBT, autologous blood and marrow transplantation; EDAP, etoposide, cisplatinum, dexamethasone and ara-C; F, female; Ig, immunoglobulin; L-PAM + ADR, melphalan and adriamycin; M, male; MCNU, ranimustine; MP, melphalan and prednisolone; PBSCT, peripheral blood stem cell transplant; VAD, vincristine, doxorubicin and dexamethasone; VCAD, vincristine, cyclophosphamide, adriamycin and dexamethasone; VCAP, vincristine, cyclophosphamide, doxorubicin and prednisolone; VMP, vincristine, melphalan and prednisolone.

than 25% of all nucleated bone marrow cells, 'severe' if the myeloma cells accounted for over 75% of all nucleated bone marrow cells, and 'moderate' if the invasion was between 'mild' and 'severe'.

Estimation of VEGF and FGF-2 concentrations in MM patients' plasma

Plasma samples were collected from 10 patients with refractory myeloma (cases 2–11) before and after 2–4 weeks of thalidomide administration. FGF-2 and VEGF were measured with an enzyme-linked immunosorbent assay (ELISA) system (R&D Systems, Minneapolis, MN, USA). Briefly, the plasma was collected and, after adding EDTA as an anticoagulant, was stored at –80°C. Patients' samples were applied to microtiterplates coated with a specific monoclonal antibody, and they were incubated at room temperature for 2 h. The plates were then washed three times and, after adding peroxidase-conjugated secondary polyclonal antibodies specific for the primary antibodies to the wells, they were incubated at room temperature for 2 h. After washing the wells, a substrate solution was added and the intensity of the blue color products was measured at 450 nm with a microplate reader (Bio-Rad, Hercules, CA, USA). The limit of detection of FGF-2 and VEGF in plasma was 1 pg/mL and 15.6 pg/mL, respectively. The FGF-2 and VEGF concentrations were considered elevated if they exceeded the highest value in the healthy control group. The cutoff values of FGF-2 and VEGF were 7.67 pg/mL and 38.3 pg/mL, respectively.

Thalidomide treatment and assessment of therapeutic effectiveness

Thalidomide was supplied by Sociedade Farmaceutic Brasifa Ltda. (Rio de Janeiro, Brazil) and administered *per os* at a dose of 200 mg/day for 7 days. No chemotherapeutic agents, including steroids, or radiotherapy was administered during thalidomide treatment. Certain supportive therapies, including blood transfusion, granulocyte colony-stimulating factor (G-CSF), supplemental gamma globulin, and/or pamidronate disodium administration were permitted concomitantly. If no serious side-effects were observed during the first week, the dose of thalidomide was increased to 400 mg and continued as a maintenance dose. When side-effects, such as granulocytopenia, were observed in patients after administering the increased dose of thalidomide, the dose was decreased to 200 mg/day. The effectiveness of thalidomide was evaluated by classifying the patients according to their response into the following groups: a responsive group, with a more than 30% decrease in serum M-protein or daily urine Bence Jones protein concentration sustained for at least 4 weeks; a stable group, with a less than 25% change in M-protein level; and a progressive group, with a more than 30% increase in M-protein level.

RESULTS

Microvessel density of the bone marrow of untreated patients

The MVD of the bone marrow of the 51 patients with MM or MGUS and the six control patients with non-hematological disorders is shown in Fig. 1. The typical histological findings of the bone marrow observed while counting microvessels are shown in Fig. 2. The MVD of the bone marrow in the control group was 20.4–70.9 vessels/mm^2 ($n = 6$, 43.5 ± 20.3 vessels/mm^2). The MVD of the bone marrow of MGUS patients varied widely, from 38.9 to 133.3 vessels/mm^2 ($n = 9$, 78.2 ± 30.1 vessels/mm^2), and the range in the MM patients was 38.9–264.8 vessels/mm^2 ($n = 42$, 111.1 ± 60.1 vessels/mm^2). Thus, the MVD of the BM of the MM patients was

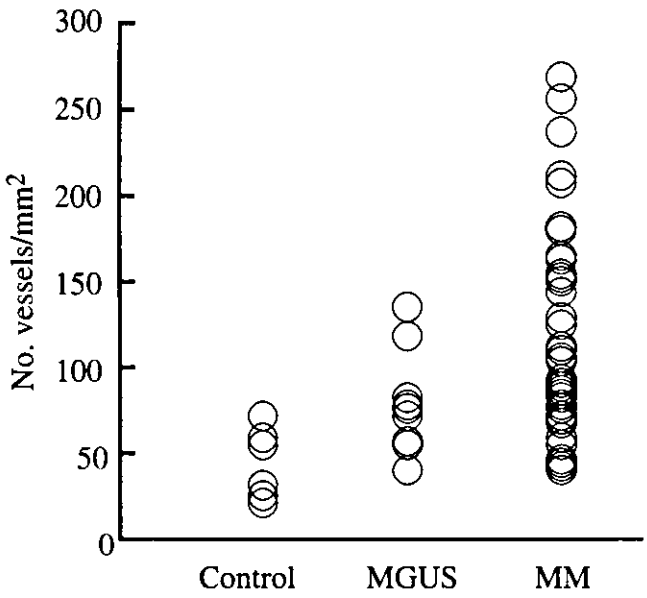

Figure 1 Microvessel density (MVD) of the bone marrow of untreated multiple myeloma (MM) patients. The MVD of the bone marrow of 51 patients and six non-hematological control patients are shown. The MVD was calculated as the number of CD34-positive microvessels observed in five fields (area of each field: 1.08 mm^2) in the bone marrow under the 80x lens of a light microscope. The MVD was 20.4–70.9 vessels/mm^2 in the control group ($n = 6$), 38.9–133.3 vessels/mm^2 in the monoclonal gammopathy of undetermined significance (MGUS) patients ($n = 9$), and 38.9–264.8 vessels/mm^2 in the MM patients ($n = 42$).

higher than in the controls; however, the increases in MVD in the MM and MGUS patients' bone marrow were not statistically significant compared with the controls.

Representative histological findings in the bone marrow of an untreated MM patient and normal bone marrow are shown in Fig. 2. Myeloma cell invasion in the bone marrow was graded by examination of HE-stained sections (Fig. 2a–d) and sections immunohistochemically stained with antiplasma cell antibody VS38c (Fig. 2e–h). There were no differences between the numbers of CD34-positive microvessels in the bone marrow with 'mild' invasion by myeloma cells and in normal bone marrow; however, there were clear increases in the number of microvessels in the bone marrow with a 'moderate' or 'severe' invasion by myeloma cells (Fig. 1). The marrow space of the bone marrow with 'severe' invasion had been replaced by numerous infiltrating myeloma cells accompanied by fibrosis. There was a marked increase in the number of microvessels in the bone marrow with a 'severe' invasion compared with normal bone marrow.

To evaluate the tendency toward increased angiogenesis in the bone marrow of MM patients statistically, we examined the MVD values of bone marrow with mild, moderate, and severe invasion by myeloma cells, and normal bone marrow. The results showed that MVD increased with the grade of myeloma cell invasion (Fig. 3). The mean MVD of normal bone marrow and the mild invasion cases was 43.5 and 79.5 vessels/mm^2, respectively, as opposed to 113.1 and 167.4 vessels/mm^2 in the moderate and severe invasion cases, respectively. The MVD of bone marrow in the moderate invasion cases and the severe invasion cases was significantly higher than in normal bone marrow ($P < 0.05$ and $P < 0.005$, respectively).

Thalidomide treatment and angiogenesis in bone marrow

Eleven refractory cases (six females and five males) that had been treated with traditional chemotherapy were treated with thalidomide (Table 2). Figure 4a shows the concentrations of M-protein in serum (cases 1–3, 5–11) and urine (case 4) before and after thalidomide treatment. Cases in which the M-protein concentration in serum or urine decreased to below 70% after thalidomide treatment were defined as 'responsive' cases. Cases with over 130% of the initial M-protein concentration after treatment were defined as 'progressive' cases. Cases with 70–130% of the initial concentration of M-protein after treatment were defined as 'stable' cases. Of the 11 cases treated with thalidomide, seven (64%) were 'responsive', three were 'stable', and one was 'progressive'. The urine concentration of M-protein in case 4 was 6010 mg/dL before treatment with thalidomide, and decreased to 1050 mg/dL after 4 weeks of treatment. In case 1, the concentration of serum M-protein changed from 5940 mg/dL to 2394 mg/dL after administration of thalidomide. In the 'responsive' cases, the grade of plasma cell invasion in the bone marrow was lower or unchanged after treatment. In the 'stable' and 'progressive' group, the grade of plasma cell invasion was unchanged or had increased after thalidomide treatment. There was an obvious decrease in the degree of bone marrow invasion in some of the patients in whom thalidomide treatment was effective.

Figure 4b shows the MVD of the bone marrow before and after thalidomide therapy. In the seven 'responsive' cases, MVD decreased in three cases (cases 6, 9 and 11) and increased in three cases (cases 1, 4, and 5) and was stable in one case (case 10). The MVD of case 10 was lower than the other cases before and after the treatment with thalidomide. The MVD increased in all of the 'stable' cases (cases 3, 7 and 8), but decreased in the 'progressive' case (case 2). No tendency toward a correlation between the effectiveness of thalidomide and the changes in the MVD of the bone marrow after thalidomide treatment was found.

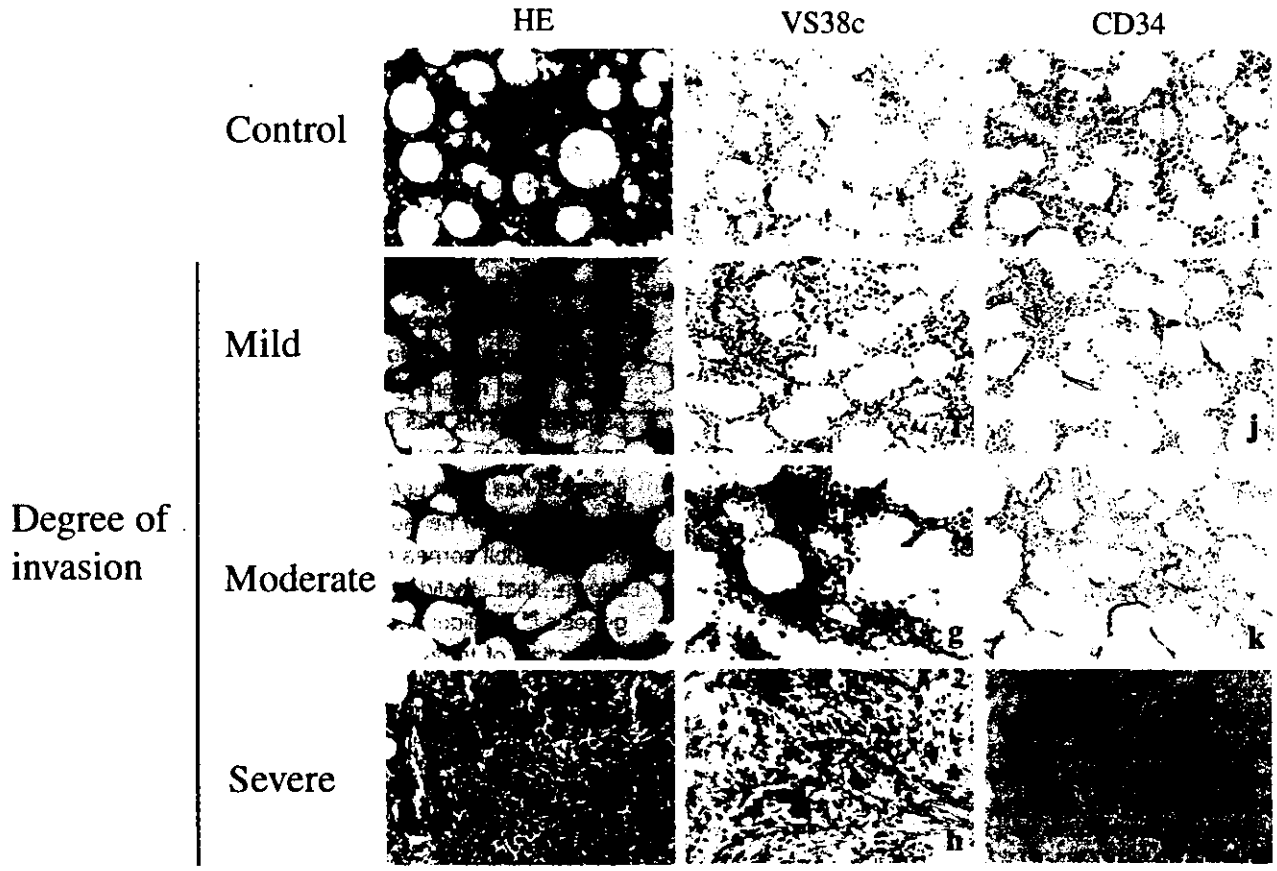

Figure 2 Grading of myeloma cell invasion and angiogenesis in the bone marrow of untreated multiple myeloma (MM) patients. Representative histologies of the bone marrow of an untreated MM patient and normal bone marrow are shown. Myeloma cell invasion in the bone marrow was graded by examining (**a,b,c,d**) sections stained with hematoxylin–eosin (HE) and (**e,f,g,h**) sections immunohistochemically stained with antiplasma cell antibody, VS38c. (**i,j,k,l**) Immunohistochemical staining with anti-CD34 antibody was performed to visualize the blood vessels. The number of microvessels in the bone marrow with 'moderate' or 'severe' myeloma cell invasion was obviously increased (**k,l**). In the bone marrow with 'severe' invasion, the marrow space was replaced by numerous infiltrating myeloma cells and accompanied by a fibrosis. There was a marked increase in the number of microvessels in the bone marrow with 'severe' invasion, compared with normal marrow (**i**).

Plasma FGF-2 and VEGF concentrations after thalidomide treatment

The plasma concentrations of angiogenic factors, FGF-2 (bFGF) and VEGF, were measured by ELISA in 10 patients treated with thalidomide. Before thalidomide treatment, the plasma FGF-2 concentrations in all of the cases in which FGF-2 was detectable (nine cases) exceeded the normal range (FGF-2 was not detectable in the plasma in case 4) (Fig. 5a). The highest plasma value was 278 pg/dL, in case 6. After 2–4 weeks of thalidomide treatment, the FGF-2 concentration had decreased in all nine cases, including the progressive case (case 2) with an increased serum M-protein concentration and the cases with increased MVD of the bone marrow (cases 3,5,7 and 8) after treatment with thalidomide.

Plasma VEGF concentrations were also determined by ELISA (Fig. 5b). Before the thalidomide therapy, an increased VEGF concentration of plasma was seen in nine cases, and the highest value was 208 pg/dL (case 5). In these nine cases, after 2–4 weeks of thalidomide treatment, a decrease of VEGF concentration was observed in eight cases, and the plasma VEGF concentration in six of these eight cases was within the normal range. These decreases in plasma FGF-2 or VEGF concentration may also have been caused by thalidomide.

Representative histological sections of bone marrow before and after thalidomide treatment in case 9, a 'responsive' case, are shown in Fig. 6. The myeloma cell invasion in the bone marrow had improved after treatment, and the number of CD34-positive microvessels had decreased. Immunohistochemistry with anti-FGF-2 antibody revealed that the cytoplasm of many hematopoietic cells, including myeloma cells, was positive (Fig. 6). There were no significant changes in the FGF-2 staining pattern after thalidomide treatment, despite the decreased concentration of FGF-2 after treat-

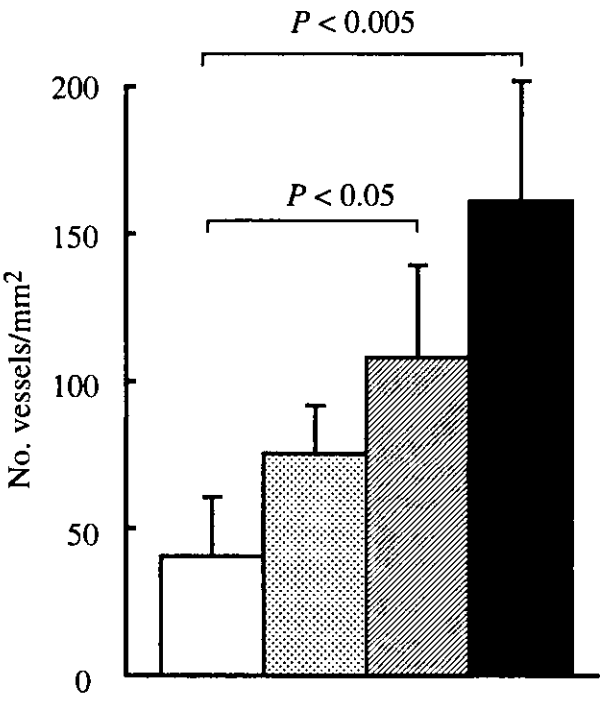

Figure 3 Increased microvessel density (MVD) in the bone marrow of multiple myeloma (MM) patients. The MVD was measured in the bone marrow with mild, moderate and severe invasion of myeloma cells and in the normal bone marrow in order to statistically evaluate the tendency toward increased angiogenesis in the bone marrow of MM patients. The MVD increased with the grade of myeloma cell invasion. The mean MVD in normal bone marrow and mild invasion cases was 43.5 and 79.5 vessels/mm^2, respectively, as opposed to 113.1 and 167.4 vessels/mm^2 in the moderate and severe invasion cases, respectively. The increased MVD in the moderate and severe invasion cases were significant compared with normal bone marrow ($P < 0.05$ and $P < 0.005$, respectively). (□), Control ($n = 6$); (▨), mild invasion ($n = 14$); (▨), moderate invasion ($n = 28$); and (■) severe invasion ($n = 9$).

ment. In contrast, FGF Receptor 1 was also widely expressed by hematopoietic cells, including myeloma cells (Fig. 6). No alterations in FGF Receptor 1 expression were seen after treatment.

DISCUSSION

The angiogenesis in solid tumors has been thought to play a role in tumor growth, invasion and metastasis.[31] In hematological malignancies, the tumor cells invade the bone marrow space and proliferate, and they replace the normal hematopoietic area because the bone marrow space is limited by the surrounding trabeculae of bone. The results of the present study showed that the MVD of the bone marrow of MM patients was higher than in the healthy controls, and greater angiogenesis was observed in MM patients with higher grades of myeloma cell invasion of the bone marrow. These findings suggest that the relationship between angiogenesis and development of MM is similar to their relationship in solid tumors.[31] Although it is not yet clear whether angiogenesis is indispensable to the pathogenesis of the disease, if angiogenesis is necessary for the development of MM, inhibition of angiogenesis may be a useful means of treatment.[19]

Vacca *et al.* reported a positive correlation between angiogenesis and the disease activity of MM.[32] Furthermore, the increased angiogenesis in bone marrow and increased levels of stimulators of angiogenesis, including FGF-2, VEGF and HGF, have recently been reported in human leukemia patients.[6,33] This has led to discussion of the possibility of antiangiogenic therapy for hematological malignancies. Thalidomide has been used to treat some MM patients as a new therapy for MM because it has an antiangiogenic effect. By using a rabbit cornea micropocket assay, D'Amato *et al.* has shown that thalidomide inhibits FGF-2-induced angiogenesis.[24] Thalidomide has also been reported to suppress production of tumor necrosis factor alpha by macrophages and to stimulate production of interleukin-2, -4, -10, and IFNγ.[34–37] These immunomodulating functions of thalidomide may contribute to the suppression of the survival and/or growth of myeloma cells. Tosi *et al.* have reported that thalidomide may suppress the progression of MM via impaired production of VEGF by myeloma cells.[38]

In the present study, we have shown that thalidomide may be effective for impairing tumor angiogenesis in the bone marrow of MM patients whose disease is refractory to conventional chemotherapy and that thalidomide reduced the plasma FGF-2 and VEGF level in almost all refractory MM cases. The cause of the decreased level of FGF-2 after thalidomide administration is unknown.

In the present study, we considered the relationship between plasma angiogenic factor (FGF-2, VEGF) level and MVD in the bone marrow of the refractory MM cases treated with thalidomide. Increased MVD was observed in the bone marrow after administration of thalidomide in some patients despite the depressed disease activity and the decreased concentrations of FGF-2 and VEGF. This discrepancy may be caused by the assessment procedure for tumor angiogenesis in the bone marrow. Singhal *et al.* also could not demonstrate a clear relationship between the bone marrow MVD and the response to the treatment with thalidomide in myeloma.[39] Hlatky *et al.* has stated that the efficacy of antiangiogenic agents cannot be simply visualized by alterations in MVD during treatment because the MVD may be outward and influenced by shrinkage, necrosis or apoptosis of the tumor.[40]

Immunohistochemistry showed that many of the hematopoietic cells and myeloma cells produced the FGF-2 protein. The FGF-2 receptors are also expressed in hematopoietic cells and myeloma cells. These results may show an auto-

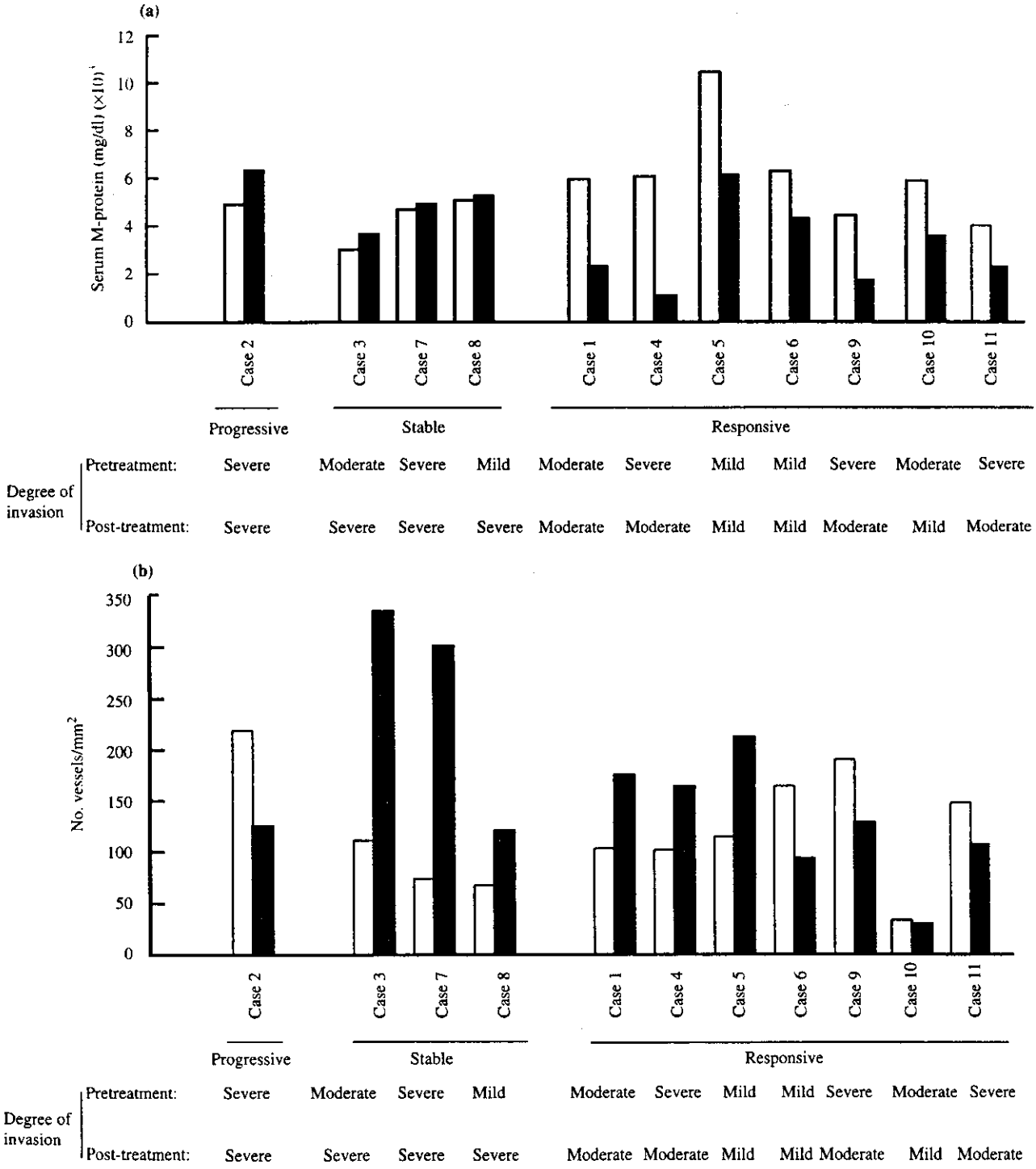

Figure 4 Effect of thalidomide treatment and change of microvessel density (MVD) of the bone marrow. (**a**) Changes in serum M-protein after thalidomide treatment. The changes in concentration of M-protein in serum (cases 1–3, 5–11) and urine (case 4) after thalidomide administration are shown. The cases were classified into three groups according to the effect of thalidomide: 'responsive'; 'stable'; and 'progressive', based on the degree of change in M-protein concentration. There were seven 'responsive' cases, three 'stable' cases, and one 'progressive' case. (**b**) Changes in MVD of the bone marrow after thalidomide treatment. The MVD of the bone marrow before and after thalidomide treatment are shown. In the 'responsive' group, MVD decreased in four cases (cases 6, 9, 10 and 11) and increased in three cases (cases 1, 4 and 5). The MVD increased in all of the 'stable' cases (cases 3, 7 and 8), but decreased in the 'progressive' case (case 2) despite the increased disease activity. (□), Pretreatment of thalidomide; (■), post-treatment of thalidomide.

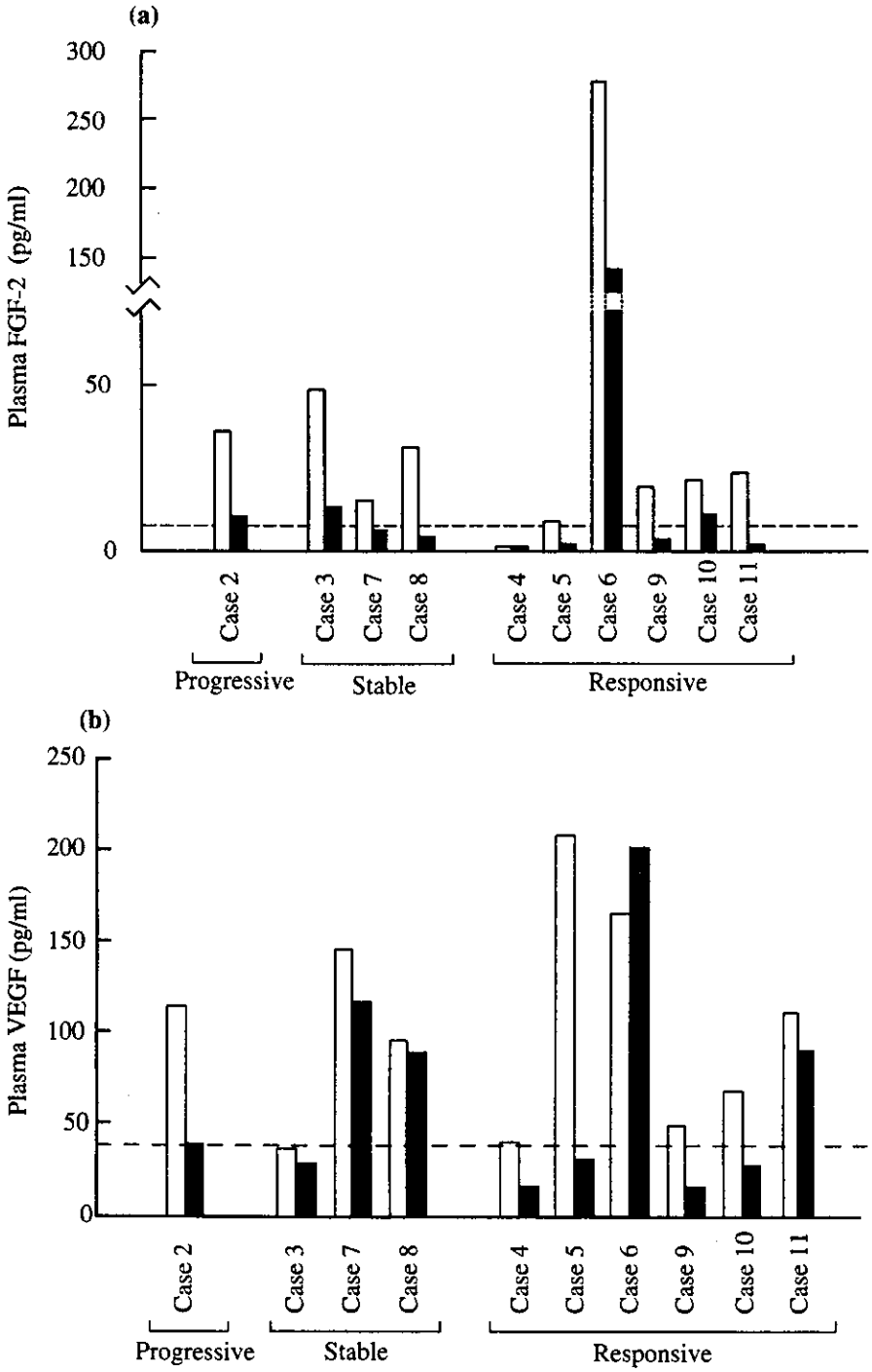

Figure 5 Plasma fibroblast growth factor (FGF-2) and vascular endothelial growth factor (VEGF) concentrations of multiple myeloma (MM) patients before and after thalidomide treatment. The concentrations of FGF-2 and VEGF were determined in 10 of the 11 cases by enzyme-linked immunosorbent assay. (**a**) Plasma FGF-2 concentrations. Before thalidomide treatment, the FGF-2 concentration in all cases in which FGF-2 was detectable (9 cases) was higher than in the healthy subjects. The highest value was 278 pg/dL, in case 8. The FGF-2 concentration decreased in all cases after thalidomide treatment, and in five cases (cases 5, 7, 8, 9 and 11) it decreased to below the upper limit in the healthy subjects. FGF-2 was not detectable in case 4. (**b**) Plasma VEGF concentration. Before thalidomide administration, the VEGF concentration in eight cases (cases 2, 5, 6, 7, 8, 9, 10 and 11) was higher than in the healthy subjects. The highest value was 208 pg/dL, in case 5. After thalidomide treatment, a decrease in VEGF concentration was observed in eight cases, and in five cases it decreased to below the upper limit in the healthy subjects. (---), Average of plasma cytokine; (□), pretreatment of thalidomide; (■), post-treatment of thalidomide.

crine loop in which the FGF-2 produced by myeloma cells affects the growth or survival of the myeloma cell. The high concentration of FGF-2 in the patients' plasma and the possible existence of an FGF-2 autocrine loop in myeloma cells suggests the possibility of using anti-FGF-2 and/or anti-FGF-2 receptor antibody as a new form of therapy.[41] The bone marrow specimens of the MM patients treated with thalidomide also stained with anti-VEGF antibody. However, there was no positive finding in all specimens because of the manipulation of decalcification.

In the present study, we showed that seven out of 11 refractory MM cases were responsive, three cases were stable, and one case was progressive for the treatment of thalidomide. In the three stable cases, two patients were of advanced age (cases 7 and 8). The patient in the progressive case (case 2) was previously treated with irradiation and

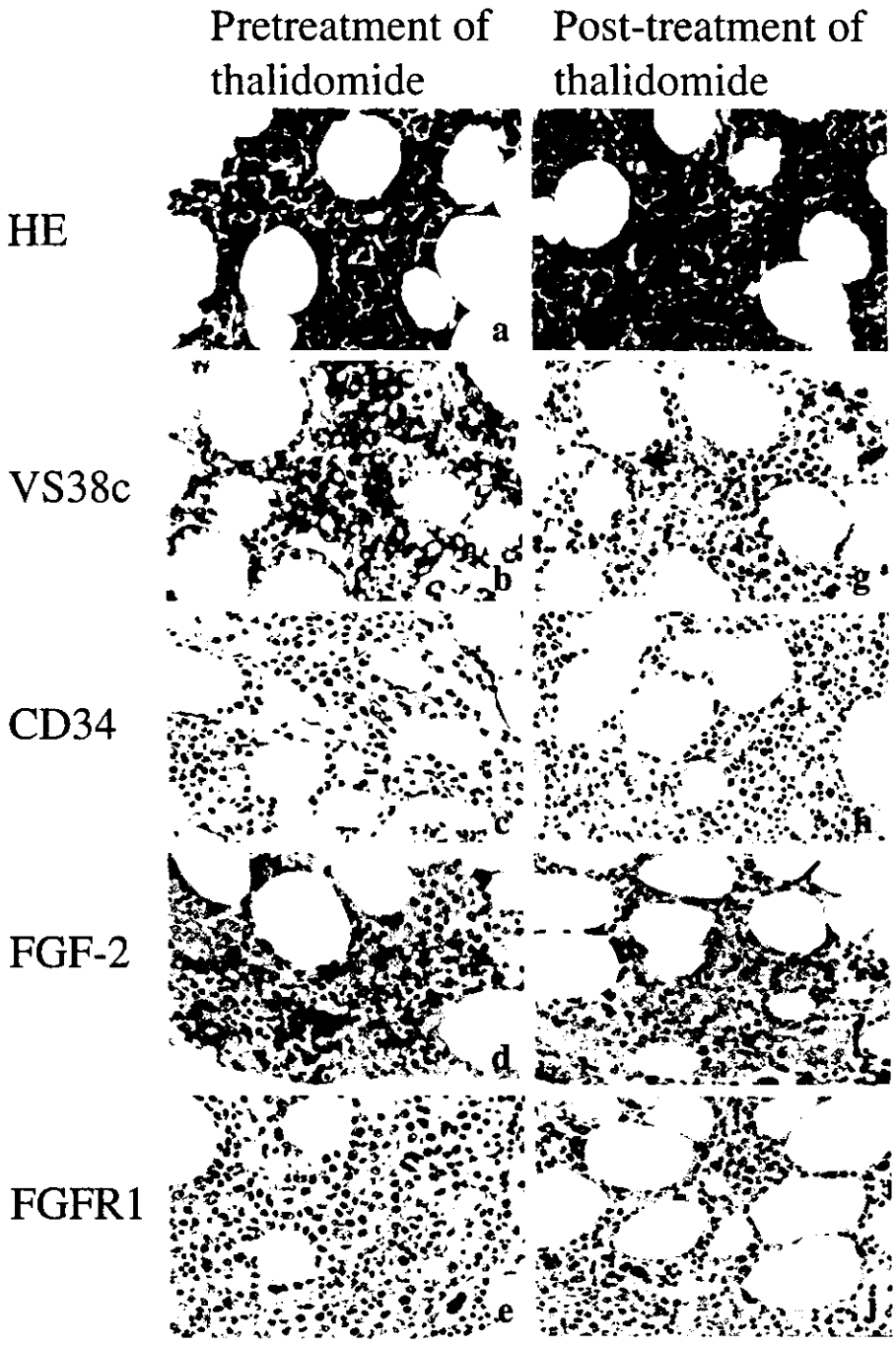

Figure 6 Histologies of the bone marrow before and after thalidomide treatment. Representative histologies of the bone marrow in case 9, a 'responsive' case, before and after thalidomide treatment are shown. (**a**,**b**,**f**,**g**) The myeloma cell invasion of the bone marrow improved after treatment. (**c**,**h**) The number of CD34-positive microvessels also decreased after treatment. Expression of fibroblast growth factor (FGF-2) was observed in the cytoplasm of hematopoietic cells and myeloma cells. (**d**,**i**) There was no significant change in the FGF-2 staining pattern after thalidomide treatment. (**e**,**j**) FGF Receptor 1 was also widely expressed in hematopoietic cells and myeloma cells, but there were no changes in its expression after treatment.

showed severe anemia before the treatment of thalidomide. Therefore, the response to the thalidomide may be influenced by age and previous therapies.

ACKNOWLEDGMENTS

This work was supported by Grants-in-Aid for Pediatric Research (12C-1) from the Ministry of Health and Welfare, research grants from the Ministry of Education and Science in Japan (10307004, 11670193, 13670190), a National Grant-in-Aid for the Establishment of a High-Tech Research Center in a Private University, the Sankyo Foundation of Life Science, Tsumura Foundation for Medical Research, Kawano Foundation for Children Cancer Research, R&D for practical use of university-based technology by matching government funds and private funds (No. 028135) and Keio Gijuku Academic Development Funds, and a special grant-in-aid for innovative and collaborative research projects at Keio University.

REFERENCES

1 Singhal S, Mehta J, Barlogie B. Advances in the treatment of multiple myeloma. *Curr Opin Hematol* 1997; **4**: 291–7.
2 Folkman J. Diagnostic and therapeutic applications of angiogenesis research. *C R Acad Sci III* 1993; **316**: 909–18.
3 Folkman J. Angiogenesis research: from laboratory to clinic. *Forum (Genova)* 1999; **9**: 59–62.
4 Folkman J. Angiogenesis-dependent diseases. *Semin Oncol* 2001; **28**: 536–42.
5 List AF. Vascular endothelial growth factor signaling pathway as an emerging target in hematologic malignancies. *Oncologist* 2001; **6**: 24–31.
6 Sezer O, Jakob C, Eucker J *et al.* Serum levels of the angiogenic cytokines basic fibroblast growth factor (bFGF), vascular endothelial growth factor (VEGF) and hepatocyte growth factor (HGF) in multiple myeloma. *Eur J Haematol* 2001; **66**: 83–8.
7 Koch AE, Polverini PJ, Kunkel SL *et al.* Interleukin-8 as a macrophage-derived mediator of angiogenesis. *Science* 1992; **258**: 1798–801.
8 Kim S, Harris M, Varner JA. Regulation of integrin alpha vbeta 3-mediated endothelial cell migration and angiogenesis by integrin alpha5beta1 and protein kinase A. *J Biol Chem* 2000; **275**: 33920–8.
9 Beck L Jr, & D'Amore PA. Vascular development: cellular and molecular regulation. *Faseb J* 1997; **11**: 365–73.
10 Kraft A, Weindel K, Ochs A *et al.* Vascular endothelial growth factor in the sera and effusions of patients with malignant and nonmalignant disease. *Cancer* 1999; **85**: 178–87.
11 Perez-Atayde AR, Sallan SE, Tedrow U, Connors S, Allred E, Folkman J. Spectrum of tumor angiogenesis in the bone marrow of children with acute lymphoblastic leukemia. *Am J Pathol* 1997; **150**: 815–21.
12 Nguyen M, Watanabe H, Budson AE, Richie JP, Folkman J. Elevated levels of the angiogenic peptide basic fibroblast growth factor in urine of bladder cancer patients. *J Natl Cancer Inst* 1993; **85**: 241–2.
13 Fiedler W, Graeven U, Ergun S *et al.* Vascular endothelial growth factor, a possible paracrine growth factor in human acute myeloid leukemia. *Blood* 1997; **89**: 1870–75.
14 Garland JM, Kumar S, Heagerty A. Angiogenesis in chronic myelogenous leukaemia. *Lancet* 2000; **356**: 1026–7.
15 Kini AR, Kay NE, Peterson LC. Increased bone marrow angiogenesis in B cell chronic lymphocytic leukemia. *Leukemia* 2000; **14**: 1414–18.
16 Aguayo A, Manshouri T, O'Brien S *et al.* Clinical relevance of Flt1 and Tie1 angiogenesis receptors expression in B-cell chronic lymphocytic leukemia (CLL). *Leuk Res* 2001; **25**: 279–85.
17 Albitar M. Angiogenesis in acute myeloid leukemia and myelodysplastic syndrome. *Acta Haematol* 2001; **106**: 170–76.
18 Stasi R, Amadori S. The role of angiogenesis in hematologic malignancies. *J Hematother Stem Cell Res* 2002; **11**: 49–68.
19 Vacca A, Ribatti D, Roncali L *et al.* Bone marrow angiogenesis and progression in multiple myeloma. *Br J Haematol* 1994; **87**: 503–8.
20 McCredie J. Mechanism of the teratogenic effect of thalidomide. *Med Hypotheses* 1976; **2**: 63–9.
21 Levy L, Fasal P, Levan NE, Freedman RI. Treatment of erythema nodosum leprosum with thalidomide. *Lancet* 1973; **2**: 324–5.
22 Cole CH, Rogers PC, Pritchard S, Phillips G, Chan KW. Thalidomide in the management of chronic graft-versus-host disease in children following bone marrow transplantation. *Bone Marrow Transplant* 1994; **14**: 937–42.
23 Wettstein AR, Meagher AP. Thalidomide in Crohn's disease. *Lancet* 1997; **350**: 1445–6.
24 D'Amato RJ, Loughnan MS, Flynn E, Folkman J. Thalidomide is an inhibitor of angiogenesis. *Proc Natl Acad Sci USA* 1994; **91**: 4082–5.
25 Rajkumar SV, Witzig TE. A review of angiogenesis and antiangiogenic therapy with thalidomide in multiple myeloma. *Cancer Treat Rev* 2000; **26**: 351–62.
26 Sato N, Hattori Y, Wenlin D *et al.* Elevated level of plasma basic fibroblast growth factor in multiple myeloma correlates with increased disease activity. *Jpn J Cancer Res* 2002; **93**: 459–66.
27 Kakimoto T, Hattori Y, Okamoto S *et al.* Thalidomide for the treatment of refractory multiple myeloma: association of plasma concentrations of thalidomide and angiogenic growth factors with clinical outcome. *Jpn J Cancer Res* 2002; **93**: 1029–36.
28 Palmer M, Belch A, Brox L, Pollock E, Koch M. Are the current criteria for response useful in the management of multiple myeloma? *J Clin Oncol* 1987; **5**: 1373–7.
29 Durie BG, Salmon SE. A clinical staging system for multiple myeloma. Correlation of measured myeloma cell mass with presenting clinical features, response to treatment, and survival. *Cancer* 1975; **36**: 842–54.
30 Hattori Y, Itoh H, Uchino S *et al.* Immunohistochemical detection of K-sam protein in stomach cancer. *Clin Cancer Res* 1996; **2**: 1373–81.
31 Folkman J. Tumor angiogenesis: therapeutic implications. *N Engl J Med* 1971; **285**: 1182–6.
32 Vacca A, Ribatti D, Roccaro AM, Frigeri A, Dammacco F. Bone marrow angiogenesis in patients with active multiple myeloma. *Semin Oncol* 2001; **28**: 543–50.
33 Bellamy WT, Richter L, Frutiger Y, Grogan TM. Expression of vascular endothelial growth factor and its receptors in hematopoietic malignancies. *Cancer Res* 1999; **59**: 728–33.
34 Fazal N, Lammas DA, Raykundalia C, Bartlett R, Kumararatne DS. Effect of blocking TNF-alpha on intracellular BCG (Bacillus Calmette Guerin) growth in human monocyte-derived macrophages. *FEMS Microbiol Immunol* 1992; **5**: 337–45.
35 McHugh SM, Rifkin IR, Deighton J *et al.* The immunosuppressive drug thalidomide induces T helper cell type 2 (Th2) and concomitantly inhibits Th1 cytokine production in mitogen- and antigen-stimulated human peripheral blood mononuclear cell cultures. *Clin Exp Immunol* 1995; **99**: 160–67.
36 Shannon EJ, Sandoval F. Thalidomide increases the synthesis of IL-2 in cultures of human mononuclear cells stimulated with Concanavalin-A, Staphylococcal enterotoxin A, and purified protein derivative. *Immunopharmacology* 1995; **31**: 109–16.
37 Tramontana JM, Utaipat U, Molloy A *et al.* Thalidomide treatment reduces tumor necrosis factor alpha production and enhances weight gain in patients with pulmonary tuberculosis. *Mol Med* 1995; **1**: 384–97.
38 Tosi P, Zamagni E, Cellini C *et al.* Salvage therapy with thalidomide in patients with advanced relapsed/refractory multiple myeloma. *Haematologica* 2002; **87**: 408–14.
39 Singhal S, Mehta J, Desikan R *et al.* Antitumor activity of thalidomide in refractory multiple myeloma. *N Engl J Med* 1999; **341**: 1565–71.
40 Hlatky L, Hahnfeldt P, Folkman J. Clinical application of antiangiogenic therapy: microvessel density, what it does and doesn't tell us. *J Natl Cancer Inst* 2002; **94**: 883–93.
41 Stan AC, Nemati MN, Pietsch T, Walter GF, Dietz H. In vivo inhibition of angiogenesis and growth of the human U-87 malignant glial tumor by treatment with an antibody against basic fibroblast growth factor. *J Neurosurg* 1995; **82**: 1044–52.

Diabetologia (2004) 47:1819–1830
DOI 10.1007/s00125-004-1522-4

Diabetologia

In vivo proliferation of differentiated pancreatic islet beta cells in transgenic mice expressing mutated cyclin-dependent kinase 4

S. Hino[1, 2] · T. Yamaoka[1] · Y. Yamashita[1] · T. Yamada[3] · J. Hata[3, 4] · M. Itakura[1]

[1] Division of Genetic Information, Institute for Genome Research, The University of Tokushima, Tokushima, Japan
[2] Department of Oral and Maxillofacial Surgery, School of Medicine, Ehime University, Ehime, Japan
[3] Department of Pathology, School of Medicine, Keio University, Tokyo, Japan
[4] National Center for Child Health and Development, Tokyo, Japan

Abstract

Aims/hypothesis. It has previously been hypothesised that highly differentiated endocrine cells do not proliferate or regenerate. However, recent studies have revealed that cyclin-dependent kinase 4 (CDK4) is necessary for the proliferation of pancreatic islet beta cells. The aim of this study was to determine whether activation of CDK4 can potentially be used as a radical treatment for diabetes without malignant transformation.
Methods. We generated transgenic mice expressing mutant *CDK4* under the control of the *insulin* promoter to examine the effect of activated CDK4 overexpression in the postnatal development of pancreatic islets.
Results. In the transgenic mice, total CDK4 protein expression was increased by up to 5-fold, with a concomitant increase in CDK4 activity indicated by the detection of phosphorylated Rb protein in pancreatic islets. Histopathologically, many cells tested positive for proliferating cell nuclear antigen, and pancreatic islets displayed hyperplasia due to the extreme proliferation of beta cells containing a large number of insulin granules. Pancreatic islet alpha, delta and PP cells did not increase. Over an 18-month observation period, the transgenic mice did not develop insulinoma. Levels of expression of *GLUT1* and *c-myc* were comparable to those in the littermates of the transgenic mice. GLUT2 expression was identified in the pancreatic islets of transgenic mice. No significant differences in telomerase activities were detected between transgenic mice and their littermates. Transgenic mice were superior to their littermates in terms of glucose tolerance and insulin secretion in response to the intraperitoneal injection of glucose, and hypoglycaemia was not observed.
Conclusions/interpretation. Activated CDK4 stimulates postnatal pancreatic beta cell proliferation, during which the highly differentiated phenotypes of pancreatic islet beta cells are preserved without malignant transformation.

Keywords CDK4 · Cell differentiation · Cell proliferation · Pancreatic islet beta cell · Transgenic mice

Introduction

The balance of growth-stimulatory and growth-inhibitory signals precisely controls proliferation, growth arrest and differentiation in mammalian cells. A series of kinase complexes govern the growth-stimulatory

Received: 16 April 2004 / Accepted: 29 June 2004
Published online: 6 October 2004

M. Itakura (✉)
Division of Genetic Information,
Institute for Genome Research,
The University of Tokushima,
3-18-15, Kuramoto-cho, Tokushima 770-8503, Japan
E-mail: itakura@genome.tokushima-u.ac.jp
Tel.: +81-88-6339454, Fax: +81-88-6339455

Abbreviations: CDK, cyclin-dependent kinase · CDK4 R24C, Arg24 to Cys substituted CDK4 · DIG, digoxigenin · DTT, dithiothreitol · GST, glutathione *S*-transferase · H&E, haematoxylin and eosin · ipGTT, intraperitoneal glucose tolerance test · MEF, mouse embryonic fibroblast · PCNA, proliferating cell nuclear antigen · PP, pancreatic polypeptide · Rb, retinoblastoma protein · Tg, transgenic

signals. Each kinase complex contains a regulatory subunit (cyclin) and a catalytic subunit (cyclin-dependent kinase [CDK]), and the level of expression of cyclin and the extent of phosphorylation of CDK control its enzymatic activity. In response to mitogenic signals, cyclin D/CDK4, cyclin D/CDK6 and cyclin E/CDK2 complexes phosphorylate retinoblastoma (Rb) protein. Initially, Ser780 is phosphorylated by the cyclin D/CDK4 complex, which is required for the transition from G_1 to S phase of the cell cycle [1, 2]. The CDK inhibitors play a central role as growth-inhibitory signals that bind to the cyclin/CDK complexes and inhibit their catalytic activity, thus negatively regulating cell cycle progression. The CDK inhibitors are classified into two families based on functional and structural homologies. The INK4 family of inhibitors ($p16^{INK4a}$, $p15^{INK4b}$, $p18^{INK4c}$ and $p19^{INK4d}$) specifically bind to CDK4 and CDK6 and prevent their interaction with D-type cyclins. The Cip/Kip family is composed of $p21^{Cip1/Waf1}$, $p27^{Kip1}$ and $p57^{Kip2}$ and has a broader inhibitory profile, blocking the activities of cyclin D-, E- and A-dependent kinases [3].

It has previously been hypothesised that, like nerve cells, highly differentiated endocrine cells do not proliferate or regenerate. Advances in developmental biology and molecular biological techniques such as cell culture, transgenic (Tg) and knock-out and knock-in mice have allowed the molecular mechanisms of pancreatic development to be gradually elucidated. Recent studies have revealed that islet cells can regenerate even in adult pancreas [4]. This finding raises the possibility that impaired pancreatic islets or a decrease in the number of islet cells in diabetic patients can be restored. The targeted homozygous disruption of CDK4 ($CDK4^{-/-}$) in mice results in a dramatic reduction in the number of pancreatic beta cells and a diabetic phenotype, including hyperglycaemia, ketosis, glucosuria and polydipsia [5, 6]. Furthermore, these mice are small in size due to an overall reduction in the size of major organs, and are infertile due to defective spermatogenesis and a reduced number of Leydig cells, or limited prolactin production [5, 6]. Mouse embryonic fibroblasts (MEFs) derived from $CDK4^{-/-}$ mice proliferate in a similar manner to wild-type MEFs. However, MEFs from $CDK4^{-/-}$ mice show delayed re-entry into the S phase of the cell cycle following serum stimulation [5, 6]. Re-expression of endogenous CDK4 in beta cells by crossing $CDK4^{-/-}$ mice with transgenic mice that express the Cre recombinase under the control of the rat *insulin* promoter restores cell proliferation and normoglycaemia [7]. These results indicate that CDK4 is indispensable for normal pancreatic development. Conversely, the $CDK4^{R24C/R24C}$ knock-in mice carrying the Arg24 to Cys substituted CDK4 (CDK4 R24C) display pancreatic islet hyperplasia due to the excessive proliferation of beta cells [6]. These mice develop spontaneous multiple tumours with almost complete penetrance and increased susceptibility to chemical carcinogen-induced tumourigenesis [6, 8]. The most common neoplasias are endocrine tumours and haemangiosarcomas [8]. MEFs derived from $CDK4^{R24C/R24C}$ mice are immortal and are insensitive to contact inhibition of cell growth [8]. This mutation was first identified in patients with hereditary melanoma and causes CDK4 to lose its affinity for $p16^{INK4a}$ without affecting its ability to bind cyclin D and form a functional kinase complex [9, 10]. In contrast, this mutation does not affect the interaction of CDK4 with $p21^{Cip1/Waf1}$ or $p27^{Kip1}$ [9].

Conventional diabetes therapies are partially effective, but they are not necessarily directed toward the fundamental aetiology of the disease. Regenerative medicine is expected to provide a greater degree of physiological control of blood glucose concentrations. However, there are concerns that these therapies could cause the malignant conversion of targeted cells. To investigate these possibilities, we generated transgenic mice expressing *CDK4 R24C* under the regulation of the *insulin* promoter in pancreatic islets (CDK4 R24C-Tg mice). We examined whether CDK4 plays an important role in the fetal and postnatal development of pancreatic islets, and whether CDK4 can be used as a molecular target for the radical treatment of diabetes.

Materials and methods

Generation of transgenic mice. The construction of the expression vector including the 1.9-kb human *insulin* promoter used to generate transgenic mice has been described previously [11]. Human *CDK4 R24C* cDNA was provided by D. Beach (Howard Hughes Institute, Cold Spring Harbor, N.Y., USA) and was inserted into the cloning site flanking the exon–intron organisation and a polyadenylation signal of the rabbit *β-globin* gene. The *BssH*II-excised fragment of this vector excluding the plasmid-derived sequence was used as the transgene (Fig. 1a).

The transgene was micro-injected into male pronuclei of fertilised eggs obtained from super-ovulated BDF1 (C57BL/6 × DBA2 F1) female mice crossed with males of the same strain. Injected eggs were implanted into the oviducts of pseudopregnant female mice and allowed to develop [12]. DNA was extracted from tail snips of live offspring using the proteinase K/SDS method [11]. The integration of the transgene into the mouse genome was detected by PCR between a sense primer in exon 1 of the human *insulin* promoter (5′-GCATCAGAAGAGGCCATCAA-3′) and an antisense primer in exon 3 of the rabbit *β-globin* gene (5′-ACTCACCCTGAAGTTCTCAG-3′) and by Southern blot analysis. The *SalI–NotI* fragment of the transgene was used as a probe and compared with indicator bands of 1, 10 and 100 copies of the transgene. The F1 transgenic progeny were bred by crossing transgenic founder mice with BDF1 mice, and were used to observe phenotypes over the long term and to repeat crossing with BDF1 mice. The F2 transgenic mice and their sex-matched non-transgenic littermates (wild-type mice) were used in this study. The F2 transgenic mice were back-crossed to C57BL6 mice or DBA2 mice for four genera-

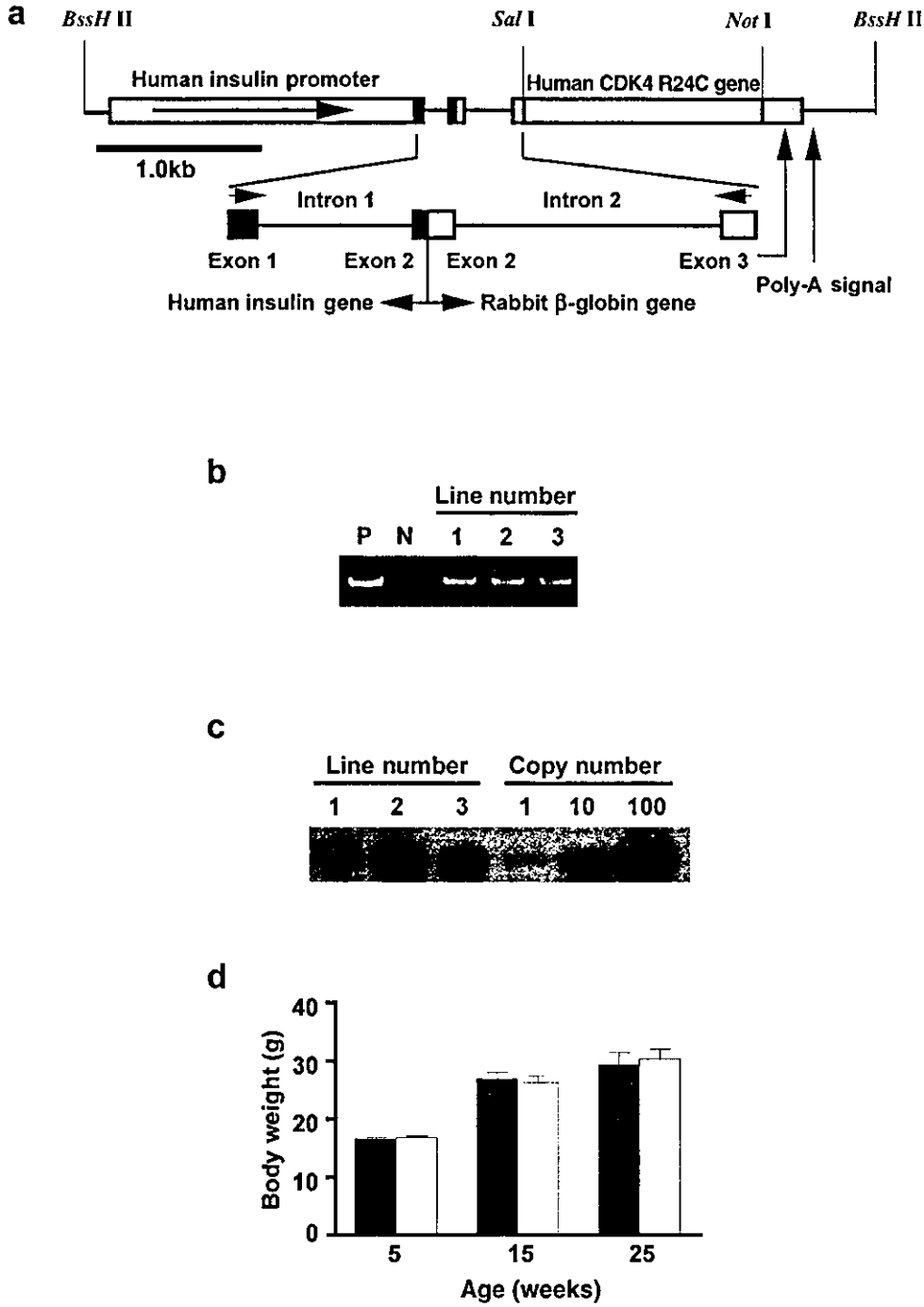

Fig. 1. Transgene construct and expression. **a.** The transgene construct used in this study. Human CDK4 R24C transgene was expressed in mouse pancreatic islets under the control of the human *insulin* promoter. **b.** In order to detect transgene-derived mRNA, a sense primer in exon 1 of the human *insulin* promoter (left horizontal arrow) and an antisense primer in exon 3 of the rabbit *β-globin* gene (right horizontal arrow) were synthesised for RT-PCR. P, positive control; N, negative control. **c.** The copy numbers of integrated transgene in lines 1 to 3 of the transgenic mice were examined by Southern blotting. **d.** Bar graph of the body weights of the mice at 5, 15 and 25 weeks of age. The results shown are the means ± SEM of values for at least 13 mice. Black bars, littermates; white bars, CDK4 R24C-Tg mice

tions. Body weight was determined weekly. All mice were supplied by CLEA Japan (Tokyo, Japan) and handled according to the "Principles of Laboratory Animal Care" (NIH Publication No. 85–23, revised 1985).

Transgene expression in pancreatic islets. Pancreatic islets were collected by the collagenase method [13, 14], total RNA was extracted with ISOGEN (Wako Pure Chemical Industries, Osaka, Japan) and reverse-transcribed by SuperScript First-strand Synthesis System (Invitrogen, Carlsbad, Calif., USA) in 20 μl of the reaction mixture. A 1-μl aliquot of the products was subjected to PCR amplification. To determine whether conditions were adequate for semi-quantitative RT-PCR, we reverse-transcribed 0.01, 0.1, 1 and 5 μg of total RNA and amplified the fragments under the same PCR conditions using 15 to 30 cycles. We used 1 μg of total RNA as a template for

reverse transcription, and the cDNA fragment was amplified by using sense and antisense primers specific to human *CDK4* (5′-TACCTCTCGATATGAGCCAG-3′ and 5′-CACCAGGGTTACCTTGATCT-3′). Sense and antisense primers to *β-actin* were used as an internal standard (5′-GTGGGCCGCTCTAGGCACCA-3′ and 5′-CGGTTGGCCTTAGGGTTCAGG-3′). After confirming the linear increase in the PCR product with increasing amounts of total RNA, we chose the middle cycle number of 15 to 30 cycles in the phase of linear logarithmic increment for each gene to semi-quantitate the mRNA expression in pancreatic islets. PCR products were separated by polyacrylamide gel electrophoresis and visualised with ethidium bromide. The expression of *amylin* (5′-TGTGCATCTCCAAACTGCCA-3′ and 5′-GATTCCCTATTTGGATCCCC-3′), *Pax4* (5′-ACACCAGGCAGCAGATTGTG-3′ and 5′-CCTGTGCGGTAGTAGCGTCC-3′), *c-myc* (5′-CGTGAACTTCACCAACAGGA-3′ and 5′-CTCTGCTGTTGCTGGTGATA-3′) and *GLUT1* (5′-GAATCGTCGTTGGCATCCTT-3′ and 5′-AGATGACACTGAGCAGCAGA-3′) was examined similarly.

Immunoprecipitation, immunoblotting and the CDK4 kinase assay. Pancreatic islets collected by the collagenase method were washed three times with ice-cold PBS and lysed in lysis buffer containing 50 mmol/l HEPES (pH 7.5), 0.1% Tween 20, 150 mmol/l NaCl, 2.5 mmol/l EGTA, 1 mmol/l dithiothreitol (DTT), 10% glycerol, complete protease inhibitor cocktail (Roche, Mannheim, Germany), 10 mmol/l β-glycerophosphate, 1 mmol/l NaF, and 0.1 mmol/l sodium orthovanadate (all phosphatase inhibitors were from Sigma, St. Louis, Mo., USA). Sonicated extracts were clarified by centrifugation and the supernatants were used as whole cell lysates [15]. The protein concentrations of the supernatants were determined by the Bradford method (Bio-Rad, Hercules, Calif., USA). The supernatants were precipitated at 4 °C for 6 h with the indicated antibody, and immunoprecipitates were isolated using protein G-agarose beads (Roche) at 4 °C for 1 h. The beads were subsequently washed four times with lysis buffer. For immunoblotting, boiling in SDS-PAGE sample buffer denatured whole cell lysates or immunoprecipitated beads. Denatured proteins in the supernatants were separated by SDS-PAGE and transferred onto Immobilon-P membranes (Millipore, Bedford, Mass., USA). Membranes were probed with antibodies to CDK4, Rb, β-tubulin (Pharmingen, San Diego, Calif., USA) or Rb phosphorylated at Ser780 (Cell Signaling Technology, Beverly, Mass., USA). Horseradish peroxidase-conjugated secondary antibody (Amersham Pharmacia Biotech, Little Chalfont, UK) and the Enhanced Chemiluminescence Detection System (Amersham Pharmacia Biotech) were used for signal detection.

The assay used to assess CDK4 kinase activity was as described previously [16]. In brief, glutathione *S*-transferase (GST)-tagged Rb proteins derived from pGEX.3X.mRb.C′-ter vector (a kind gift by Dr. H. Matsushime, Yamanouchi Pharmaceutical Company, Tokyo, Japan) were expressed in *Escherichia coli* BL21 (pLysS) and affinity purified using glutathione-Sepharose CL-4B (Amersham Pharmacia Biotech), according to the manufacturer's instructions. Whole cell lysate was incubated with an antibody to CDK4 at 4 °C for 6 h. Antigen–antibody complexes were precipitated with protein G-agarose beads at 4 °C for 1 h, which were then washed four times with lysis buffer. Recovered CDK4–cyclin D complexes were incubated at 30 °C for 30 min in 20 µl of kinase buffer (50 mmol/l HEPES [pH 8.0], 10 mmol/l $MgCl_2$, 1 mmol/l DTT, 2.5 mmol/l EGTA, 10 mmol/l β-glycerophosphate, 1 mmol/l NaF, 0.1 mmol/l sodium orthovanadate) supplemented with 20 µmol/l ATP, 3.7×10^5 Bq of [γ-^{32}P]ATP (Amersham Pharmacia Biotech) and 0.5 µg of purified GST-Rb substrate. Reactions were stopped by boiling in sample buffer and the denatured proteins were separated by electrophoresis through a 10% polyacrylamide gel. Phosphorylated proteins were visualised by autoradiography.

Examination of proliferation and differentiation markers of pancreatic islets. For the histopathological examination, mouse pancreas was fixed with 20% formalin in PBS, embedded in paraffin, sectioned and stained with haematoxylin and eosin (H&E). For immunohistochemistry, guinea pig polyclonal antibodies for porcine insulin, glucagon, somatostatin and pancreatic polypeptide were used (DAKO Japan, Kyoto, Japan). Tumourigenesis of pancreatic islets was examined by insulin content, expression of *GLUT1*, GLUT2, *Pax4*, *c-myc* and *amylin*, with an SV-40-transformed pancreatic islet beta cell line of MIN6 used as a transformed insulinoma cell line. Fasting insulin concentration was used as an indicator of insulinoma. Mouse monoclonal antibodies were used to identify proliferating cell nuclear antigen (PCNA) (DAKO Japan) in proliferating cells and GLUT 2 in well-differentiated beta cells (Chemicon International, Temecula, Calif., USA). Quantitative analysis of the islet cell area was carried out as previously described [11].

Glucose tolerance test, HbA1c measurement, plasma insulin concentrations and insulin content in the whole pancreas. After an overnight fast, the intraperitoneal glucose tolerance test (ipGTT) was performed by intraperitoneally injecting 2 mg/g body weight of glucose in physiological saline. At 0, 30, 60 and 120 min after the injection, blood glucose concentrations were determined by the glucose oxidase method with a Diasensor (Kyoto Daiichi Kagaku, Kyoto, Japan). We measured HbA_1c by ion exchange chromatography (Nippon Chemiphar, Tokyo, Japan) according to the manufacturer's protocol. Plasma insulin concentrations were assayed using an insulin ELISA kit with a mouse insulin standard (Seikagaku Kogyo, Tokyo, Japan). To determine insulin content in the whole pancreas, each pancreas was homogenised in 4 ml of ice-cold acid-ethanol solution and insulin was extracted overnight at 4 °C. After centrifugation, the supernatant was neutralised and diluted with PBS. Insulin concentrations were assayed in samples diluted 1000- or 10,000-fold [11, 17].

Determination of telomerase activities in pancreatic islets. Telomerase activities in pancreatic islets were measured using a telomerase PCR ELISA kit (Roche). Pancreatic islets were lysed in ice-cold lysis buffer for 30 min, and 10 µg of cell extract was analysed using a modified telomeric repeat amplification protocol (TRAP) [18]. Briefly, telomeric repeats are added to a biotin-labelled primer during the first reaction, then elongation products are amplified by PCR. An aliquot of the PCR product is denatured, hybridised to a digoxigenin (DIG)-labeled telomeric repeat-specific probe and bound to a streptavidin-coated 96-well plate. The immobilised PCR product is detected with an anti-DIG-POD (peroxidase) antibody, visualised by a coloured reaction product generated using the substrate tetramethylbenzidine (TMB), and semiquantified photometrically at $A_{450\,nm}/A_{690\,nm}$.

Statistical analysis. All data are presented as means ± SEM. For comparison of two means, the Student's unpaired *t* test was used. For comparison of two ratios (Q_1, Q_2), a normal distribution curve with a mean of Q_1-Q_2 and a variance of $Q_1(1-Q_1)/n_1+Q_2(1-Q_2)/n_2$ was used. A p value less than 0.05 was considered statistically significant.

Results

Generation of CDK4 R24C transgenic mice. The transgene construct used in this study is shown in Figure 1a. Three CDK4 R24C-Tg founder mice were obtained (Fig. 1b). The transgene copy numbers of CDK4 R24C-Tg mice in lines 1 to 3 were 30, 70 and 30 respectively (Fig. 1c). The percentages of F2 transgenic mice at 5 weeks of age were 56% (63 of 112) in line 1, 54% (41 of 76) in line 2 and 47% (30 in 66) in line 3, which is proportional to Mendel's law. Body weights at the age of 5, 15 and 25 weeks are shown in Figure 1d; there were no significant differences between CDK4 R24C-Tg mice and their littermates. These results indicate that overexpressed CDK4 R24C does not affect embryogenesis and survival of the mice.

The expression of the transgene in the pancreatic islets of transgenic mice was confirmed by RT-PCR. Its expression was detected in lines 1 to 3 of CDK4 R24C-Tg mice, but was not detected in their littermates (Fig. 2a). The levels of expression of the transgene in the three lines were not always correlated with their copy numbers (Figs. 1c, 2a).

The expression of CDK4 R24C and endogenous CDK4 was examined by immunoblotting with anti-CDK4 antibody. Levels of total CDK4 expression in the pancreatic islets of CDK4 R24C-Tg mice were up to five times higher than in their littermates (Fig. 2b). Thus, the level of expression of CDK4 R24C driven by the human *insulin* promoter was approximately four times higher than that of the endogenous wild-type CDK4 (Fig. 2b). CDK4 kinase activity against recombinant GST-Rb protein substrate was clearly detected in the pancreatic islets of CDK4 R24C-Tg mice, but not in those of their littermates (Fig. 2c). We also examined the phosphorylation status of Rb by immunoblotting with antibody directed against Ser780-phosphorylated Rb. Levels of Rb expression were almost the same in the two groups of mice, but phosphorylation at Ser780 was only detected in the pancreatic islets of CDK4 R24C-Tg mice (Fig. 2d). These results suggest that the mitogenic signal is not transduced in normal pancreatic islets even in the presence of a sufficient supply of oxygen and nutrients.

Hyperplasia of pancreatic islets in CDK4 R24C transgenic mice. Haematoxylin and eosin staining of pancreases from 25-week-old mice revealed that islet area was increased in CDK4 R24C-Tg mice relative to that in their littermates (Figs. 3a, b). Islet area expressed as a percentage of the area of the whole pancreas was 10.2 times higher in the CDK4 R24C-Tg mice than in their littermates (Fig. 3e). Immunohistochemical analysis for insulin revealed that the enlargement of islet area in CDK4 R24C-Tg mice was due to the proliferation of beta cells (Figs. 3c, d). Beta cell area expressed as a percentage of the area of the whole pancreas was 14.3 times higher in CDK4 R24C-Tg mice than in their littermates (Fig. 3f). The areas of other pancreatic hormonal cells, including alpha, delta and pancreatic polypeptide (PP) cells, relative to the area of the whole pancreas were similar in the two groups of mice (Figs. 4a–m).

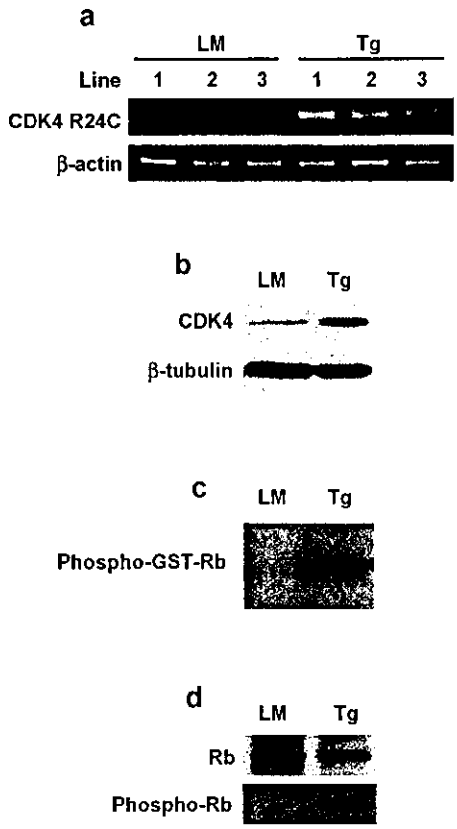

Fig. 2. CDK4 expression and its activity in CDK4 R24C-Tg mice islets. **a.** Total RNA was extracted from pancreatic islets (collected by the collagenase method) and applied to RT-PCR. In all lines of transgenic mice, RT-PCR products were amplified. **b.** Whole cell lysates were prepared from pancreatic islets as above and subjected to immunoblotting with anti-CDK4 antibody. This antibody recognises both wild-type CDK4 and CDK4 R24C. Expression of β-tubulin was measured as an internal control. **c.** CDK4 activity in pancreatic islets assayed using GST-Rb as a substrate after immunoprecipitation of CDK4. **d.** Antibody to Rb was used for immunoprecipitation, and precipitated Rb was analysed by immunoblotting with antibody specific for Ser780-phosphorylated Rb. After removing prior antibody, the total amount of precipitated Rb was determined by immunoblotting with antibody to Rb. LM, littermates; Tg, CDK4 R24C-Tg mice

In order to define the initiation of beta cell proliferation in CDK4 R24C-Tg mice, we examined the islet area in neonatal mice (Day 0) and 5-week-old mice by immunohistochemical staining for insulin. At 5 weeks, islet area was increased in CDK4 R24C-Tg mice due to the proliferation of beta cells, whereas no significant differences were observed between CDK4 R24C-Tg mice and their littermates at Day 0 (Figs. 5a–f). At 5 weeks, islet area expressed as a

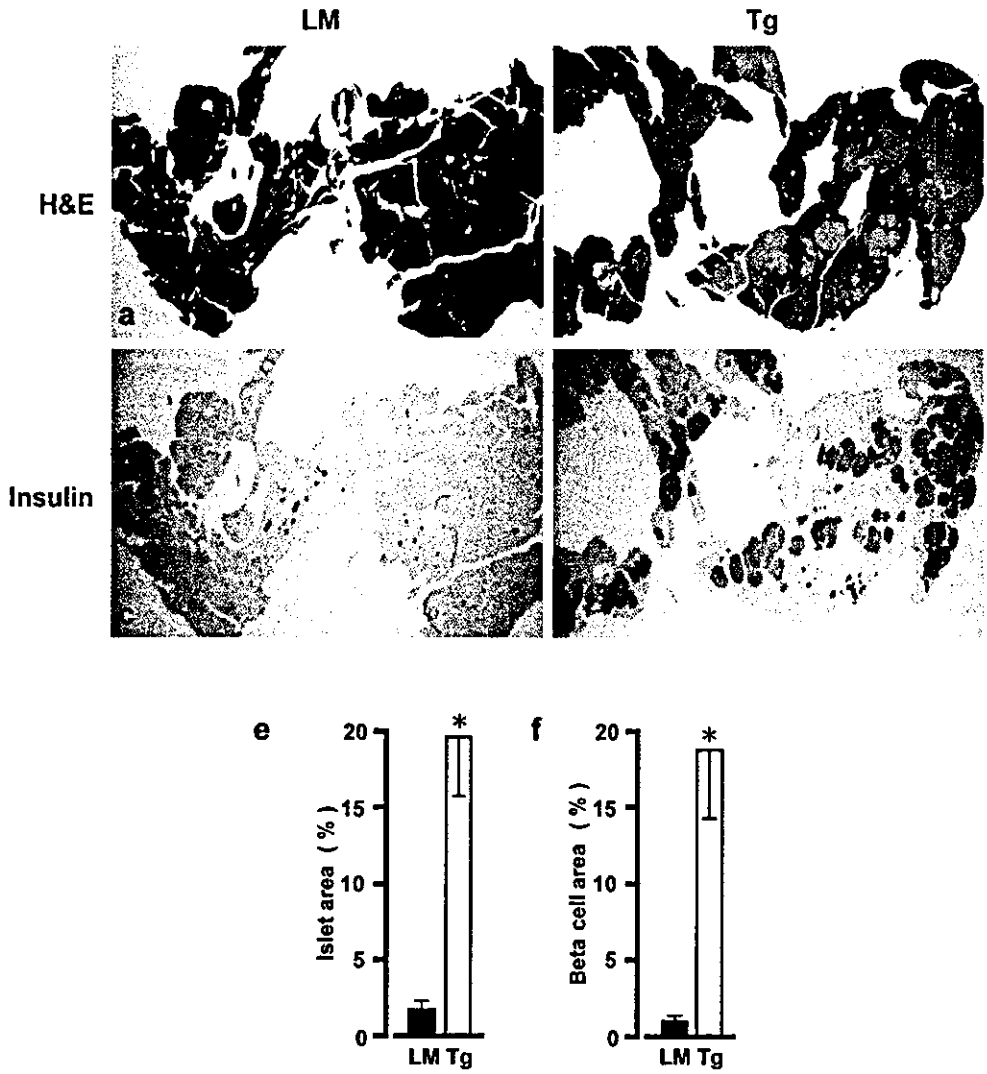

Fig. 3. Histopathological examination of pancreatic islets. At 25 weeks, sections of pancreas from littermates (**a, c**) and CDK4 R24C-Tg mice (**b, d**) were evaluated by H&E staining (**a, b**) and anti-insulin immunohistochemistry (**c, d**). Islet area (**e**) and beta cell area (**f**) relative to the area of whole pancreas (n=7 each). Both areas were significantly increased in CDK4 R24C-Tg mice (* p<0.01 vs LM). LM, littermates; Tg, CDK4 R24C-Tg mice

percentage of the area of the whole pancreas was 3.9 times higher in CDK4 R24C-Tg mice than in their littermates (Fig. 5f). There were no significant differences in the areas of other pancreatic islet endocrine cells between CDK4 R24C-Tg mice and their littermates at 5 weeks and 25 weeks (data not shown).

Glucose tolerance. In spite of the remarkable enlargement of pancreatic islets, hypoglycaemia was not observed in CDK4 R24C-Tg mice. Levels of HbA_1c in CDK4 R24C-Tg mice (1.22±0.06%, n=30) were similar to those in their littermates (1.29±0.06%, n=31). Blood glucose concentrations examined at 0, 30, 60 and 120 min after glucose injection at 5, 15 and 25 weeks of age were significantly lower in CDK4 R24C-Tg mice than in their littermates at all time points (Figs. 6a–c). Because body weight increases with age, the glucose tolerance of the littermates worsened, as indicated by the sustained high glucose levels at 60 and 120 min after glucose injection in the 15- and 25-week-old mice (Figs. 6b, c). In contrast, the glucose tolerance of the CDK4 R24C-Tg mice did not alter with age.

Insulin secretion and storage. Plasma insulin concentrations were determined at 0, 30, 60 and 120 min after glucose injection. Insulin secretion in CDK4 R24C-Tg mice at 25 weeks of age was statistically higher than that in their littermates at all time points (Fig. 6d). The insulin content of pancreases from CDK4 R24C-Tg mice (108±30 µg/pancreas g) was 2.8 times higher than that in the pancreases of their littermates (39±7 µg/pancreas g) (p<0.05, n=10 in both groups). The whole pancreatic weight was similar in both mice (data not shown).

Proliferation and differentiation of pancreatic islet beta cells. The proliferation of beta cells was con-

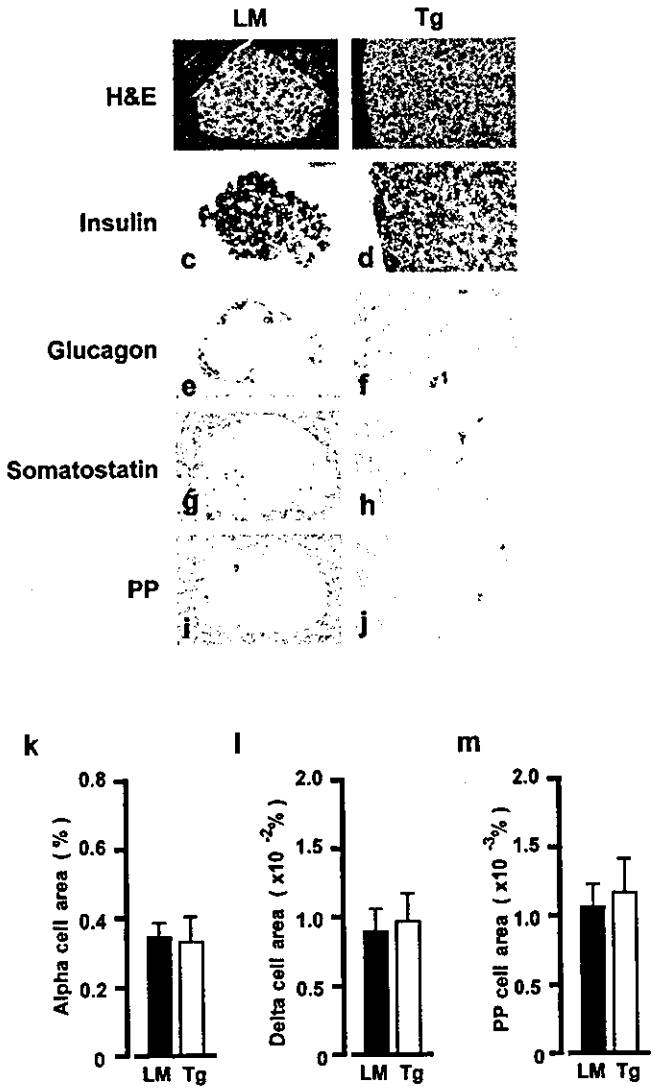

Fig. 4. Immunohistochemical analysis of pancreatic islets. Pancreata of littermates (**a, c, e, g, i**) and CDK4 R24C-Tg mice (**b, d, f, h, j**) at 25 weeks of age were examined by H&E staining (**a, b**) and immunohistochemistry against insulin (**c, d**), glucagon (**e, f**), somatostatin (**g, h**) and PP (**i, j**). The areas of alpha, delta and PP cells (**k, l, m**) relative to the area of the whole pancreas were similar in both groups of mice (n=7 each). LM, littermates; Tg, CDK4 R24C transgenic mice

firmed by positive staining against PCNA in CDK4 R24C-Tg mice (Fig. 7b). Conversely, hardly any proliferating beta cells were detected in their littermates (Fig. 7a). In order to investigate the degree of beta cell differentiation in CDK4 R24C-Tg mice, the expression of differentiation marker molecules for pancreatic islet beta cells was examined by RT-PCR and immunohistochemical analysis. Pancreatic islet beta cells in CDK4 R24C-Tg mice contained abundant insulin granules and immunohistochemical analysis for insulin showed them to be strongly stained (Figs. 3d, 4d). The level of expression of GLUT2, a marker of highly differentiated beta cells, was similar in the two groups of mice (Figs. 7c, d). Pax4 is expressed only in poorly differentiated beta cells, GLUT1 is specifically expressed in beta cells transformed into insulinoma cells, and the expression of c-myc is increased in beta cells transformed into insulinoma cells. In the present study, this pattern of expression was observed in an insulinoma cell line of MIN6 cells, but not in the pancreatic islets of CDK4 R24C-Tg mice or their littermates (Fig. 7e). The results showed that *amylin* is expressed in pancreatic islet beta cells regardless of their degree of differentiation (Fig. 7e). Moreover, insulinoma did not develop in CDK4 R24C-Tg mice over an 18-month observation period, as confirmed by histopathological analysis (data not shown).

Determination of telomerase activities. As shown in Figure 8, telomerase activities increased in the pancreatic islets of both groups of mice in an age-dependent manner. Telomerase activities in the pancreatic islets of CDK4 R24C-Tg mice were higher than in those of their littermates, but no significant differences were detected. These results suggest that the pancreatic islets did not acquire the malignant phenotype by CDK4 R24C overexpression.

Effect of genetic background on islet area and glucose tolerance. Islet area in the N4 generation of CDK4 R24C-Tg mice, back-crossed to C57BL/6 and DBA2 mice, was significantly increased in both strains in comparison with their littermates (p<0.05 for both). In their littermates, the islet area in C57BL/6 mice was significantly smaller than in DBA2 mice (p<0.01). In both strains, glucose concentrations measured at different time points during the ipGTT were significantly lower in the CDK4 R24C-Tg mice than in their littermates (p<0.05 for both). Among the littermates, glucose concentrations were significantly lower in DBA2 mice than in C57BL/6 mice (p<0.01).

Discussion

In three lines of CDK4 R24C-Tg mice, we observed a high number of copies of the transgene and generation rates of transgenic F2 mice according to Mendel's law. In other words,we have demonstrated that the expression of CDK4 R24C in pancreatic beta cells does not produce any concomitant changes in the development and growth of mice.

The over-proliferation of pancreatic islet beta cells was observed in 5-week-old CDK4 R24C-Tg mice, but not in neonatal CDK4 R24C-Tg mice. Even at 25 weeks, the beta cells of CDK4 R24C-Tg mice expressed PCNA protein, indicating that the proliferation of beta cells continues at least up to 25 weeks of age. The lack of proliferation of the beta cells of the neonatal CDK4 R24C-Tg mice may be explained by insufficient *insulin* promoter activity of the fetus. The pancreatic islets in fetal mice do not produce or

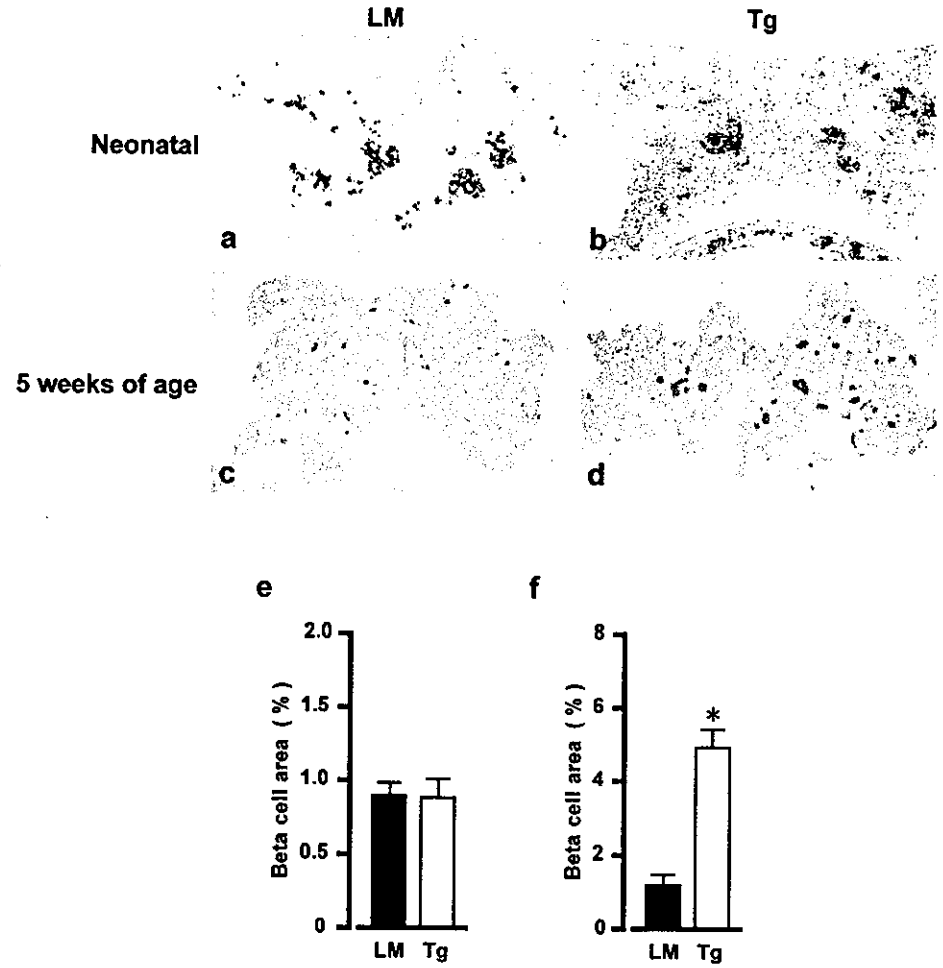

Fig. 5. Immunohistochemical analysis of pancreatic islets in neonatal mice and 5-week-old mice. Pancreata from littermates (LM) (**a, c**) and CDK4 R24C-Tg (Tg) (**b, d**) at neonatal Day 0 (**a, b**) and 5 weeks (**c, d**) were examined by immunohistochemistry for insulin. The beta cell area relative to the whole area of pancreas was determined (n=7 each). The beta cell areas were similar in the two groups of neonatal Day 0 mice (**e**), but were significantly increased in CDK4 R24C-Tg mice at 5 weeks of age (**f**) (* p<0.05 vs littermates)

secrete insulin in response to glucose stimulation, and blood glucose concentrations in fetal mice are mainly maintained by maternal insulin [19, 20, 21, 22]. Under the limited activity of the *insulin* promoter in fetal pancreatic islets, CDK4 R24C expression was not high enough to proliferate beta cells in fetal mice.

After birth, the differentiation and maturation of beta cells are induced by the demand for them to secrete insulin; thus, activation of the *insulin* promoter would be required to increase the expression of the *CDK4 R24C* transgene in order to induce the proliferation of beta cells. Beta cell areas in CDK4$^{-/-}$ and CDK4$^{R24C/R24C}$ mice at Day 15.5 of gestation and Day 5 of age have been demonstrated to be comparable to those in their littermates [7]. Furthermore, the nuclear translocation of CDK4 is developmentally regulated to coincide with the initiation of beta cell proliferation. Based on these results, another possibility is that CDK4 itself is not essential for beta cell neogenesis in the mouse embryo.

Over an 18-month observation period, insulinoma did not develop in CDK4 R24C-Tg mice as confirmed by histopathological examination. Hyperplasia of pancreatic islet beta cells was diagnosed in CDK4 R24C-Tg mice based on the following findings. Proliferation of beta cells occurred with the concomitant polyclonal enlargement of many islets. The ratio of nuclear : cytoplasmic area did not increase in the CDK4 R24C-Tg mice. The size and number of nucleoli were also similar in the two groups. In addition to the proliferating beta cells, a comparable number of alpha, delta, and PP cells were detected in pancreatic islets of CDK4 R24C-Tg mice and their littermates. Furthermore, the expression of GLUT2 (a molecular marker of highly differentiated beta cells) [23], the lack of expression of *Pax4* [24] and *GLUT1* [23] and the lack of an increase in *c-myc* expression [25, 26] indicated the absence of insulinoma development. No significant increase in telomerase activity was detected as a result of the overexpression of CDK4 R24C. In a previous study, the expression of CDK4 R24C alone had little effect on the life span of primary human keratinocytes, but simultaneous expression of

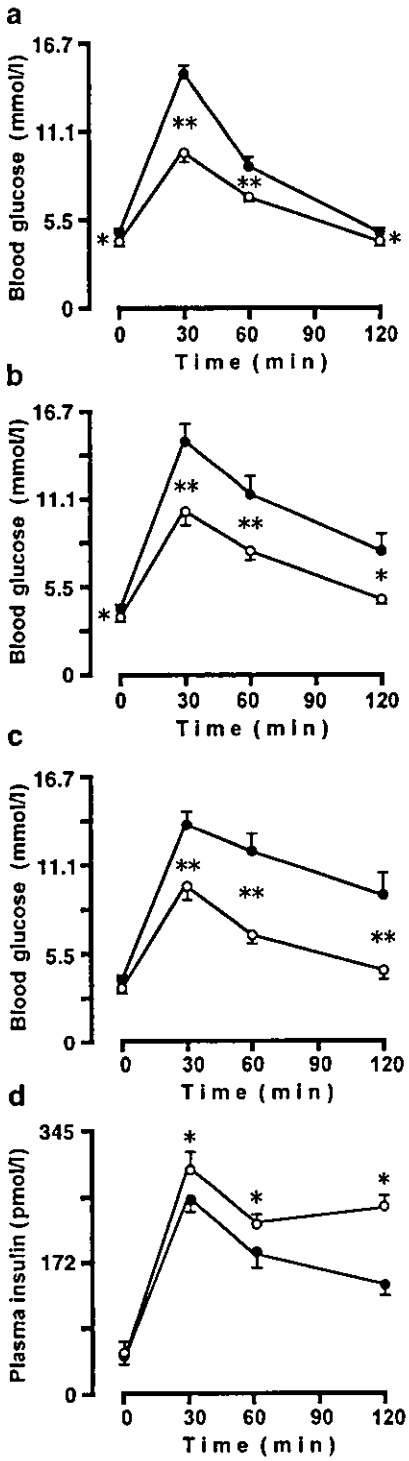

Fig. 6. Glucose levels and insulin secretion during the ipGTT. After 16 h of fasting, 2 mg/g body weight of glucose in physiological saline was intraperitoneally injected. Blood glucose concentrations were examined at 0, 30, 60 and 120 min after glucose injection at 5 (**a**), 15 (**b**) and 25 (**c**) weeks. **d.** Plasma insulin concentrations were measured at the same time points. * $p<0.05$ vs littermates; ** $p<0.01$ vs littermates. Empty circles, CDK4 R24C-Tg mice; filled circles, littermates

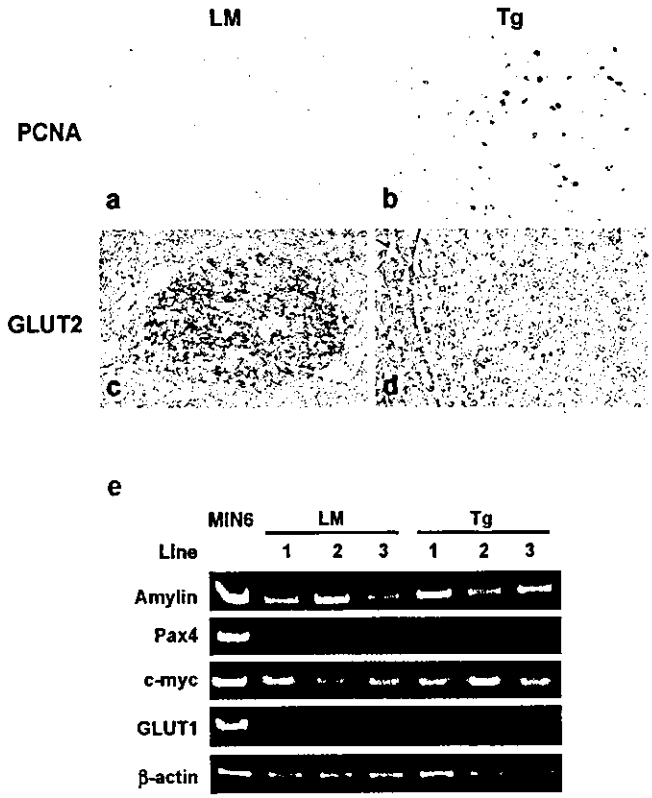

Fig. 7. Analysis of gene expression in pancreatic islets. Pancreata from littermates (**a, c**) and CDK4 R24C-Tg mice (**b, d**) at 25 weeks of age were examined by immunohistochemistry for PCNA (**a, b**) or GLUT2 (**c, d**). **e.** Islets obtained from five mice in the same line aged 20 to 25 weeks were used together for RNA extraction. Total RNA was subjected to semi-quantitative RT-PCR with specific primers for the indicated genes and for *β-actin* (internal control). MIN6 cells were used as a representative insulinoma cell line. LM, littermates; Tg, CDK4 R24C-Tg mice

dominant negative p53 permitted cells to divide beyond their normal limits [27]. In our system, the p53 pathway would suppress tumour formation by inhibiting the increase in telomerase activity and promoting the apoptosis of de-differentiated beta cells.

The results of the ipGTT confirmed that the beta cells in CDK4 R24C-Tg mice were highly differentiated. Although the early morning fasting blood glucose concentrations of CDK4 R24C-Tg mice were slightly lower than those of their littermates, they were within the normal range and were not hypoglycaemic. Fasting plasma insulin concentrations were similar in the two groups of mice. One of the diagnostic criteria for insulinoma is the presence of increasing plasma insulin concentrations even at fasting [28]. This criterion was not satisfied in CDK4 R24C-Tg mice. Furthermore, in line with the normal glucose concentrations observed in CDK4 R24C-Tg mice, insulin secretion was adequate and prompt in these mice after glucose loading. It has previously been shown that the precise regulation of insulin secretion is defective in the majority of patients with insulinoma